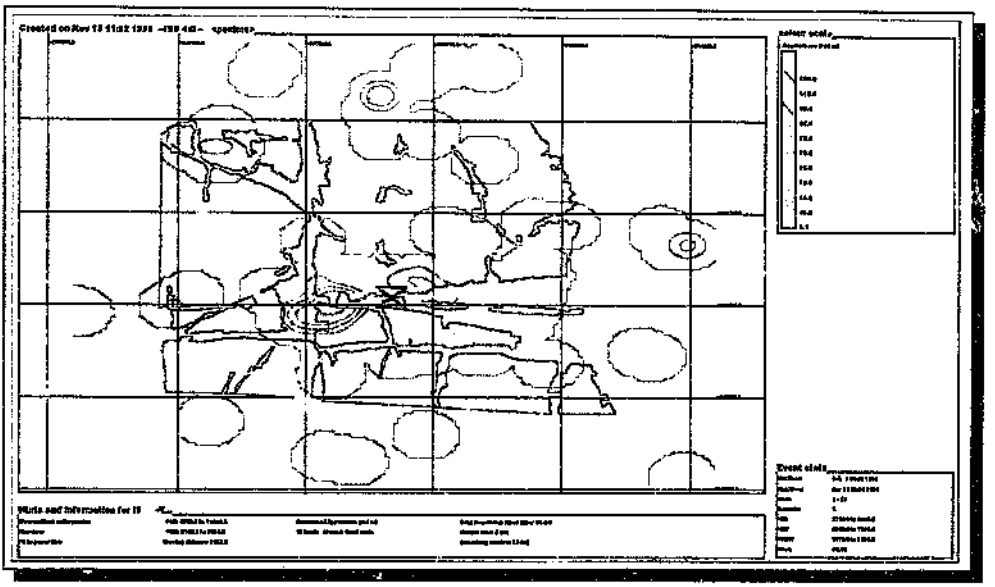

Fig. 4.104: Contours of apparent volume based on seismicity recorded in the time period 1/2/94 to 24/4/94 (approx three months leading up to event 940424, the location of which is indicated by the hourglass symbol).

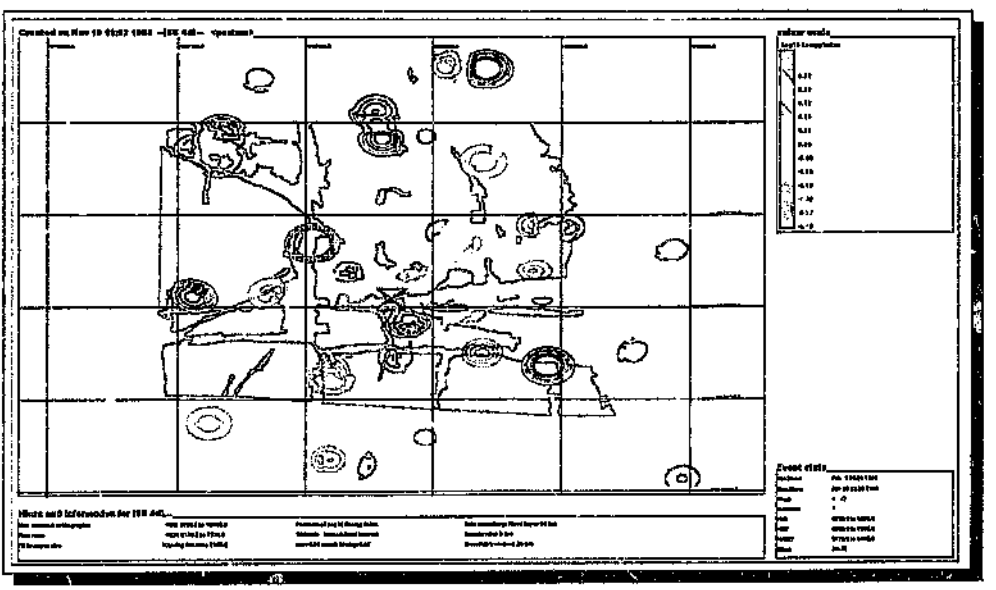

Fig. 4.105: Same as fig. 4.104; contours are of log(EI).

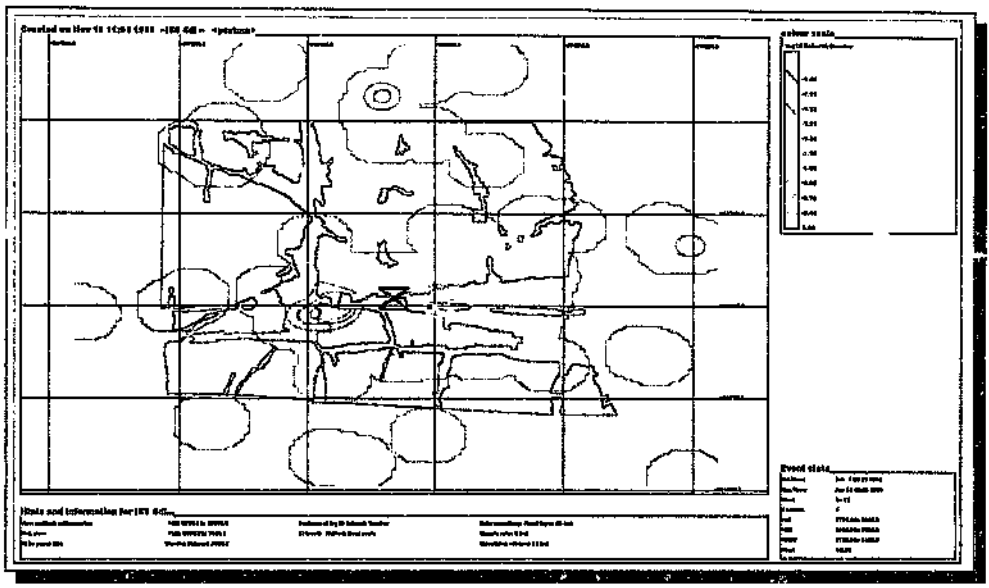

Fig. 4.106: Same as fig. 4.104; contours are of log(inv. Deborah no.).

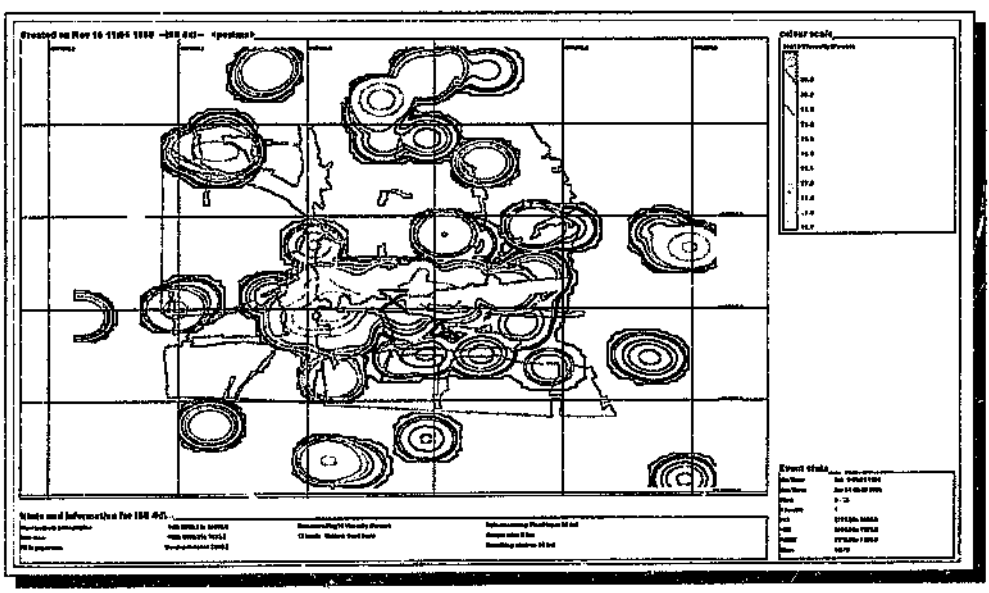

Fig. 4.107: Same as fig. 4.104; contours are of log(viscosity).

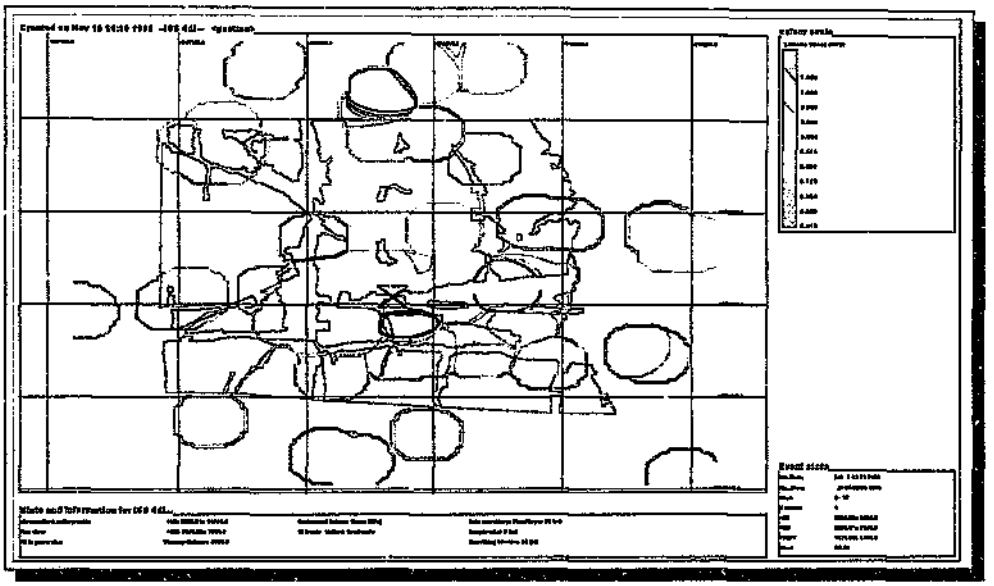

Fig. 4.108: Same as fig. 4.104; contours are of seismic stress.

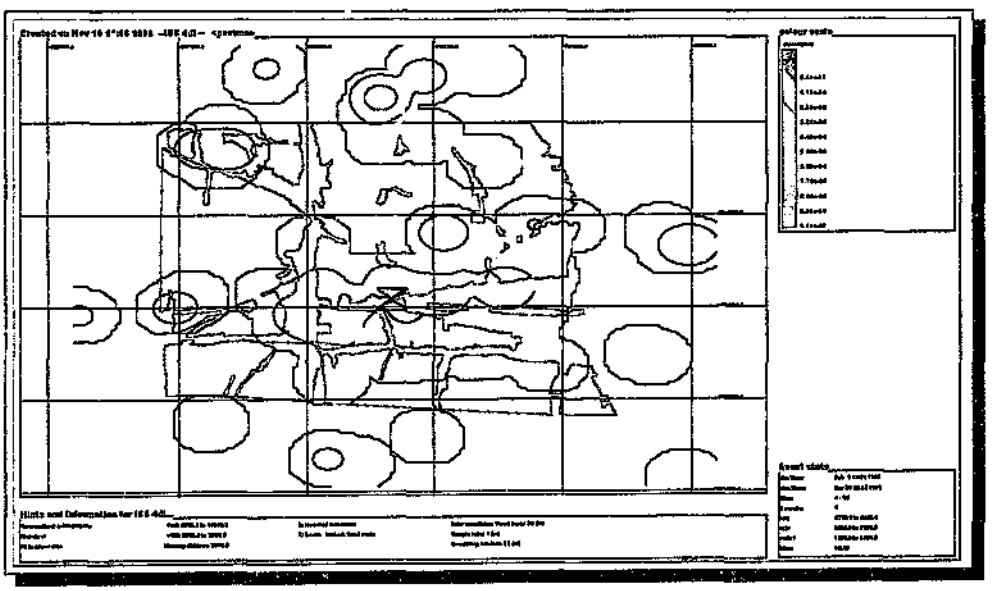

Fig. 4.109: Same as fig. 4.104; contours are of cumulative seismic strain.

APPENDIX F6

(a) Setting up of a polygon for selection of events to clarify the preparation zone of event 940513 (figs. 4.112a and 4.112b).

(b) Time-history and contour plots used in the analysis of event 940513 to identify precursors (figs. 4.113 - 4.130); Section 4.2.6, Chapter 4.

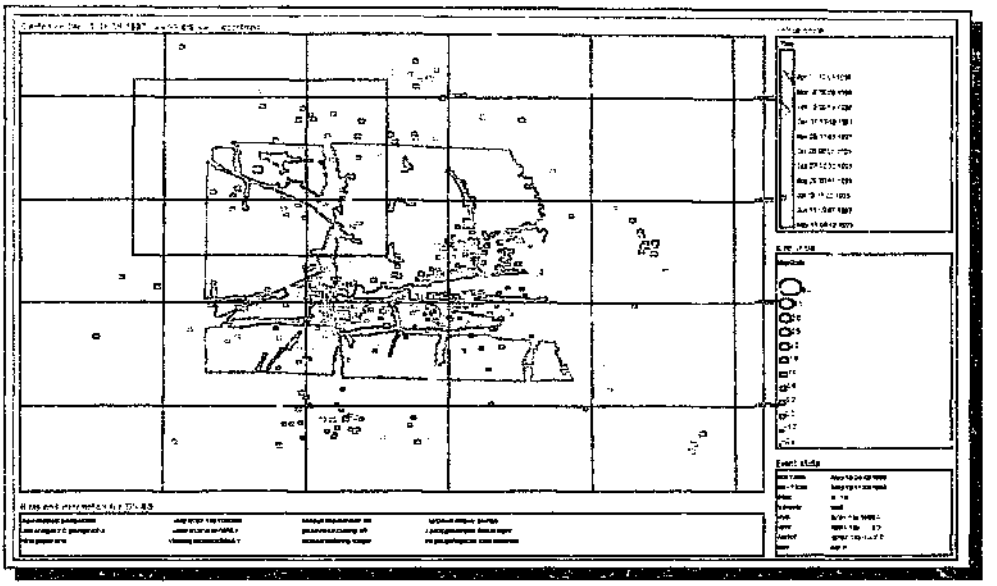

Fig. 4.112a: The rectangle in the top-left-hand corner of the Postma area denotes the polygon used for the selection of events to produce improved results in time-history analysis. Events, in this case, are represented in time (colour) and local magnitude (symbol size).

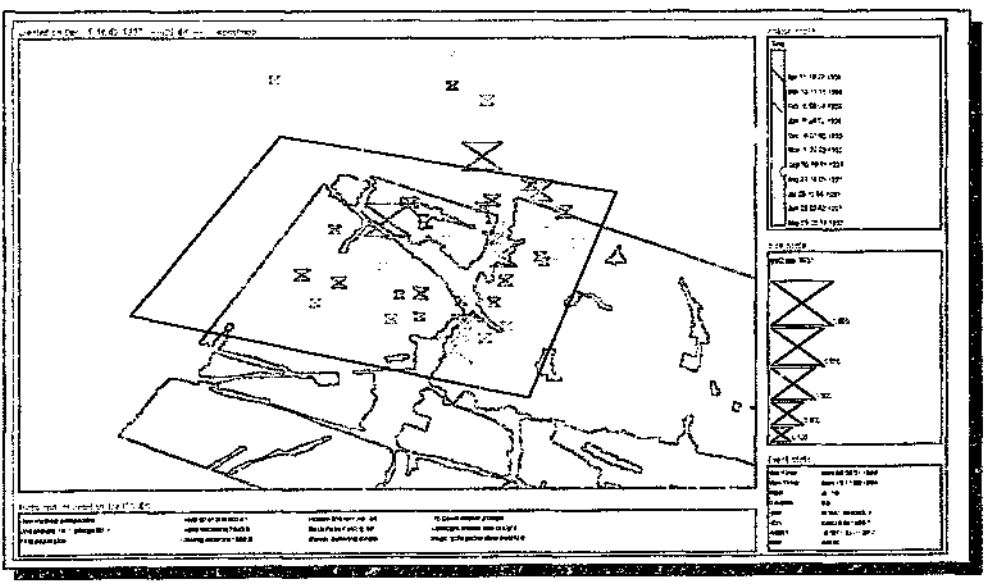

Fig. 4.112b: Perspective view of the selection of events within the polygon delivering clearer precursory changes in the variation of seismic source parameters with time. Events are denoted by apparent stress (symbol size) and time (colour).

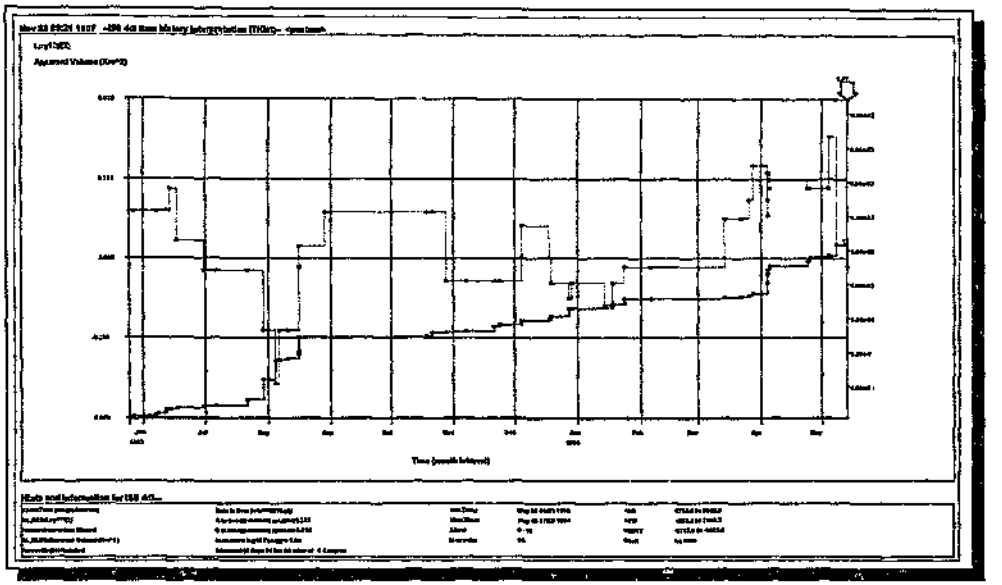

Fig. 4.113: Time-history of cumulative apparent volume and moving median log(EI) for seismicity recorded in the time period 25/5/93 to 13/5/94 (with a moving window of 5 samples and/or 10 days of data). The last arrow refers to event 940513.

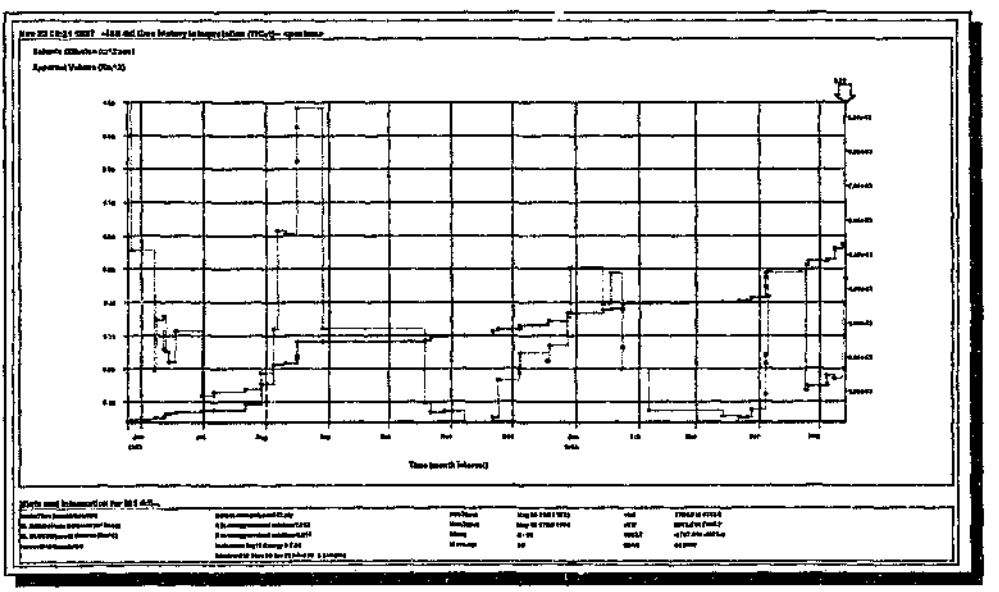

Fig. 4.114: Same as fig. 4.113, showing variation of seismic diffusion.

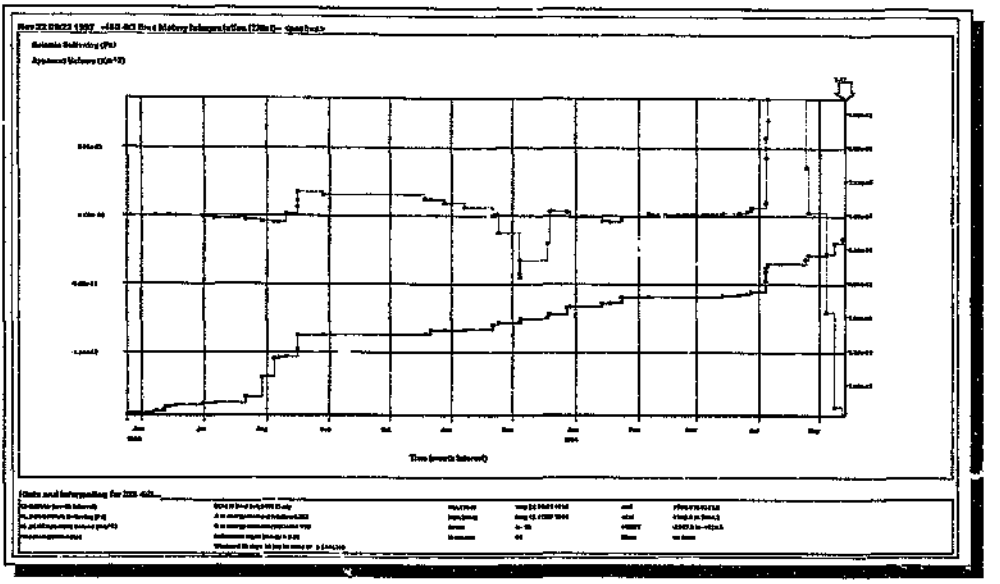

Fig. 4.115: Same as fig. 4.113, showing variation in seismic softening.

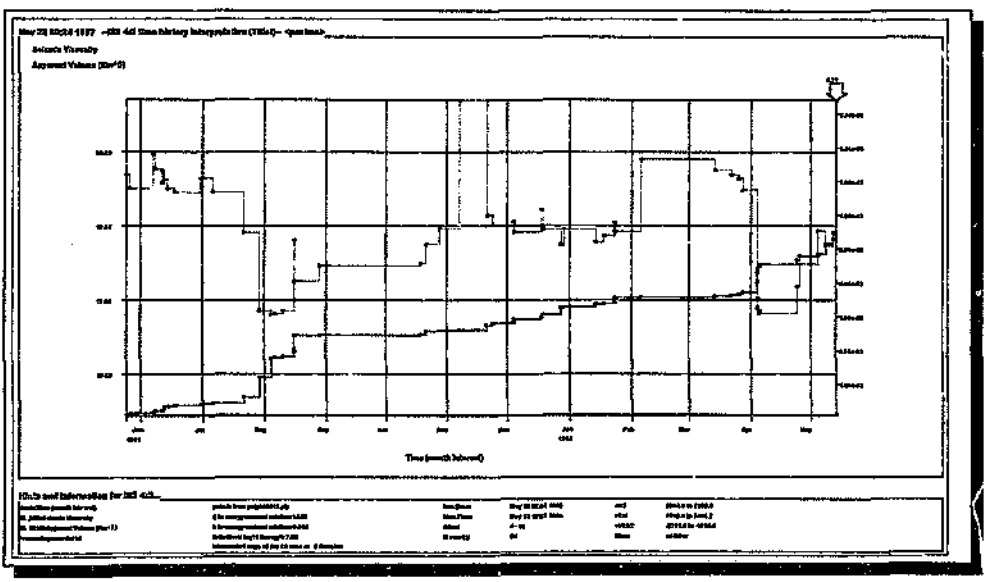

Fig. 4.116: Same as fig. 4.113, showing variation in seismic viscosity.

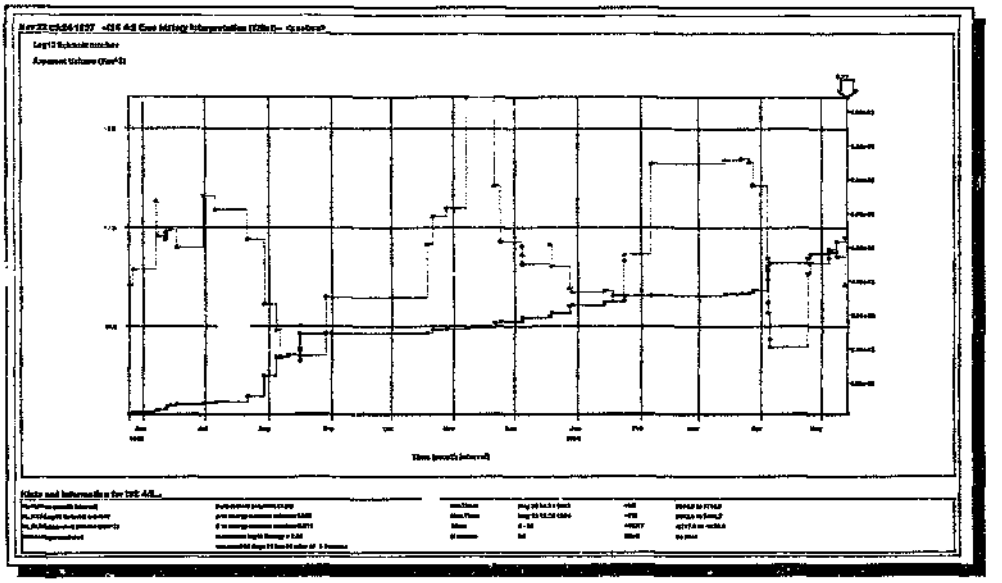

Fig. 4.117: Same as fig. 4.113, showing variation in log(seismic Schmidt no.).

Contour plots of those seismic parameters under investigation relating to the seismicity recorded 12 months before (but excluding) event 940513 (figs. 4.118 - 4.123).

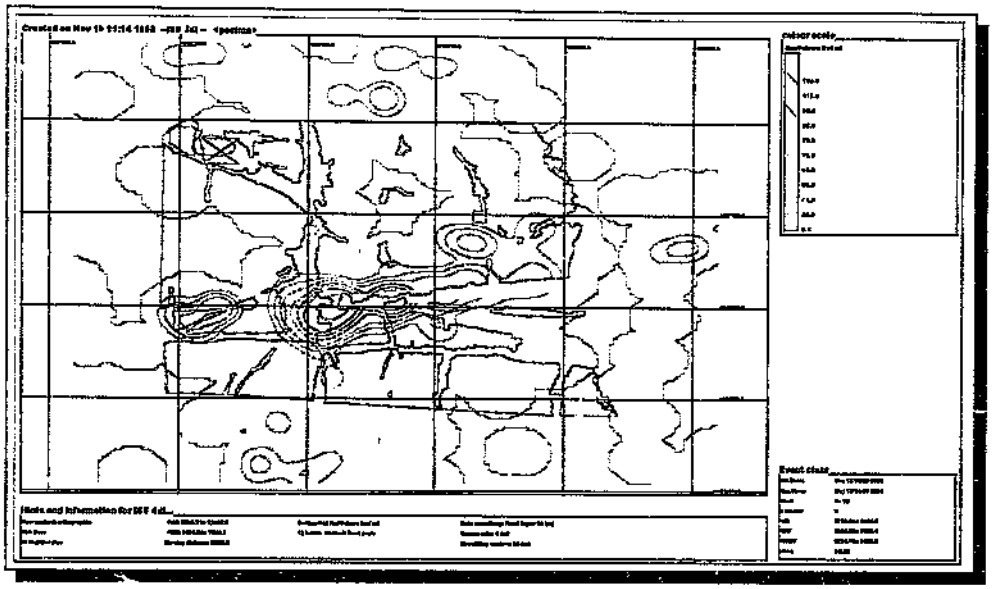

Fig. 4.118: Contours of apparent volume using seismicity recorded in the time period 13/5/93 to 13/5/94 (12 months leading up to, but excluding, event 940513, the location of which is indicated by the 'hourglass' symbol).

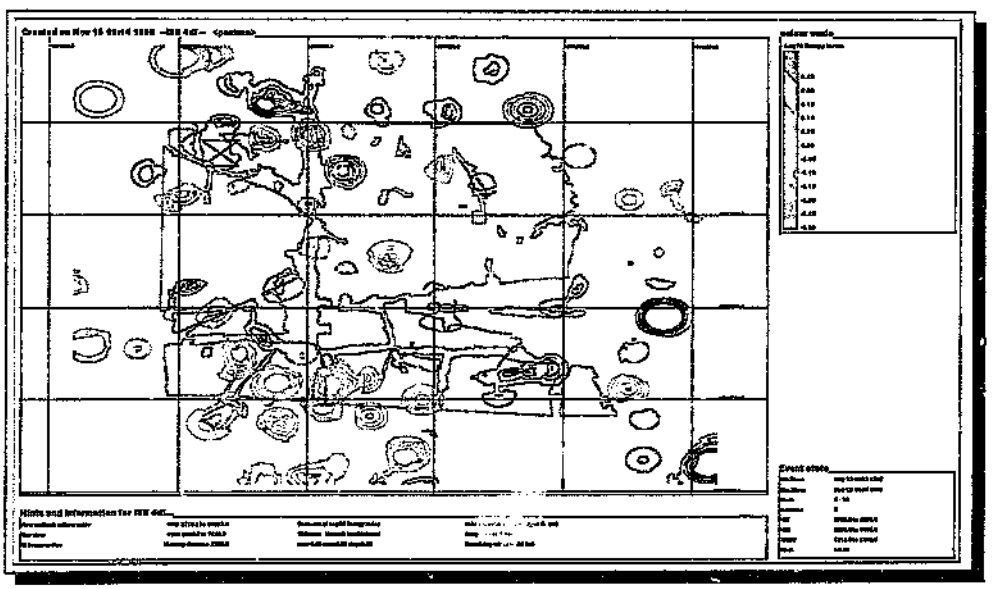

Fig. 4.119: Same as fig. 4.118, but contours are of log(EI).

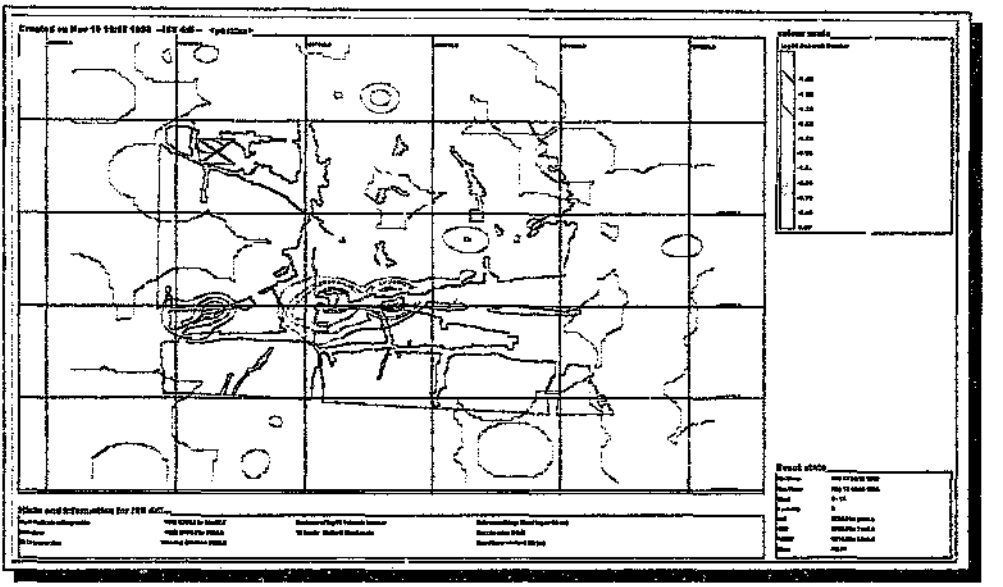

Fig. 4.120: Same as fig. 4.118; contours are of log(inv. Deborah no.).

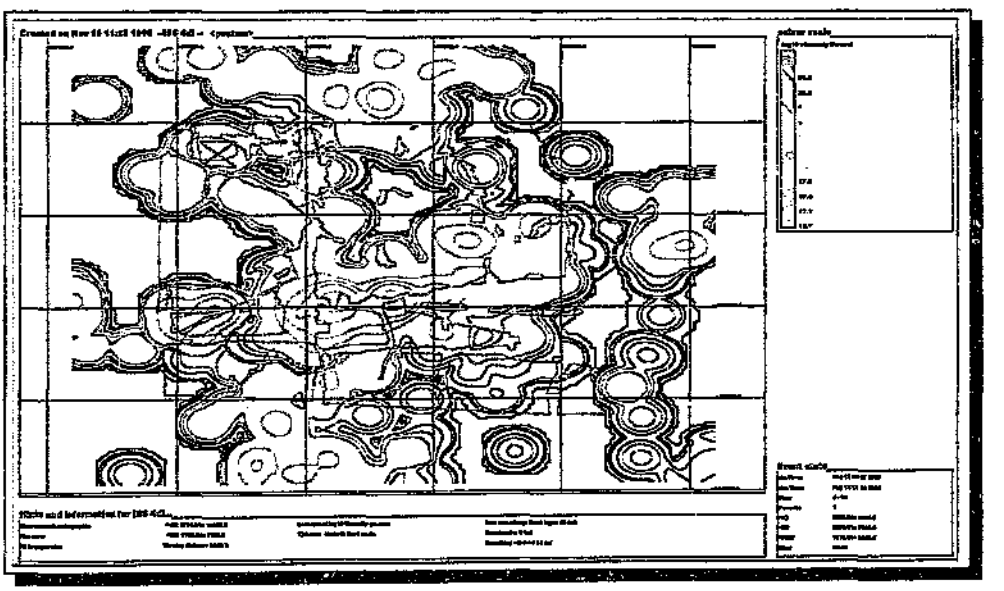

Fig. 4.121: Same as fig. 4.118; contours are of log(viscosity).

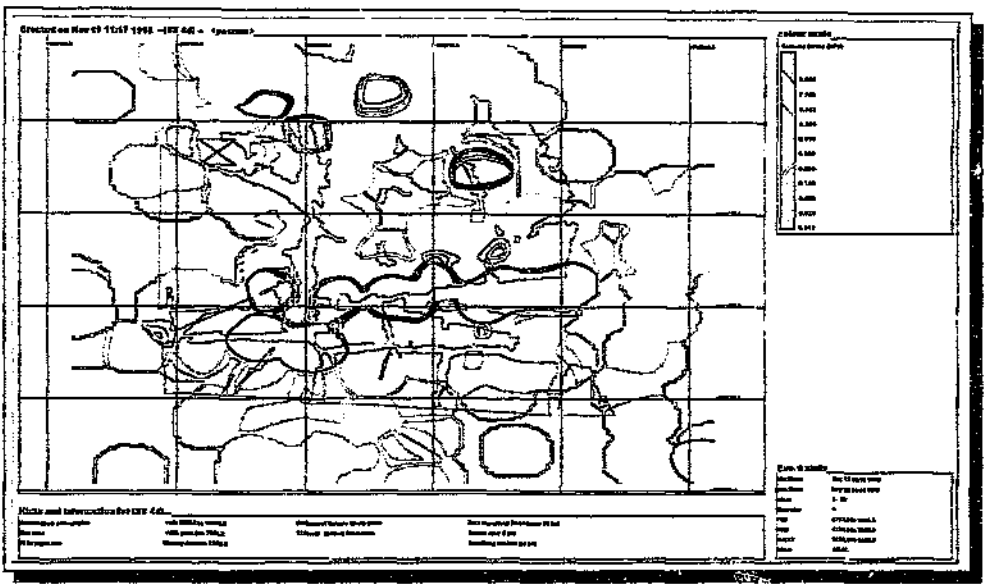

Fig. 4.122: Same as fig. 4.118; contours are of seismic stress.

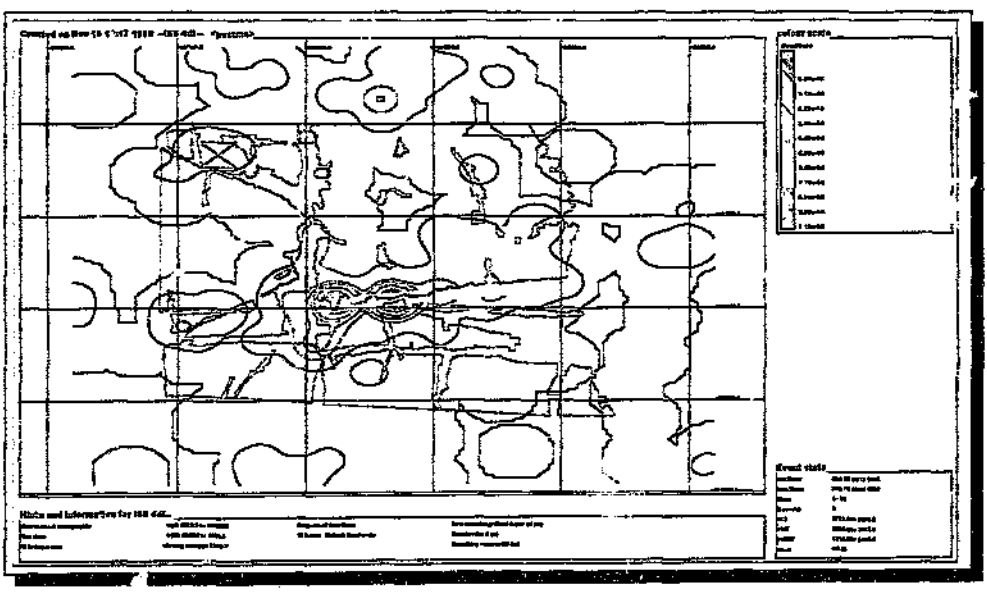

Fig. 4.123: Same as fig. 4.118; contours are of cumulative seismic strain.

Contour plots of those seismic parameters under investigation relating to the seismicity recorded 3 months before (but excluding) event 940513 (figs. 4.124 - 4.130).

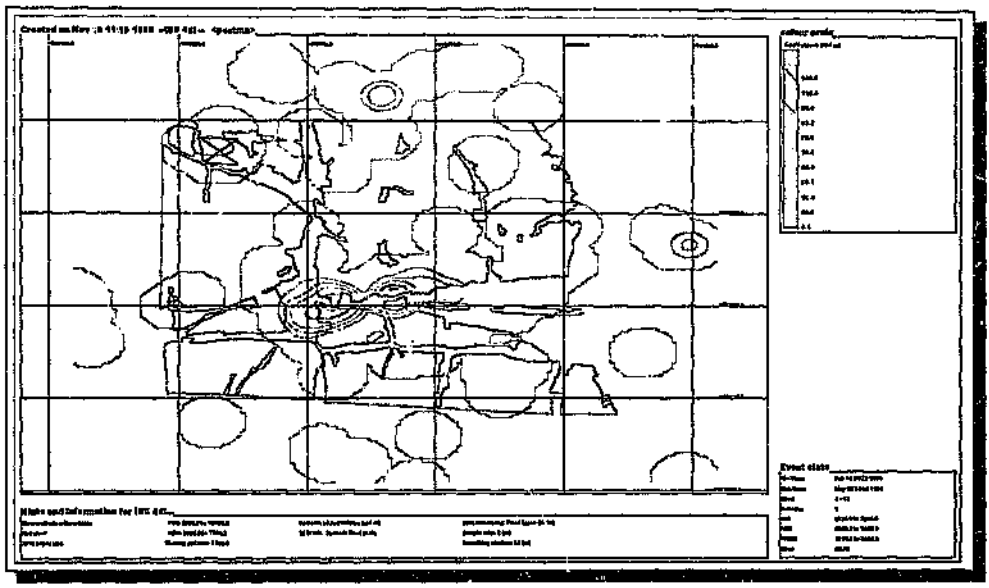

Fig. 4.124: Contours of apparent volume based on seismicity recorded in the time period 14/2/94 to 13/5/94 (three months leading up to event 940513, the location of which is indicated by the 'hourglass' symbol).

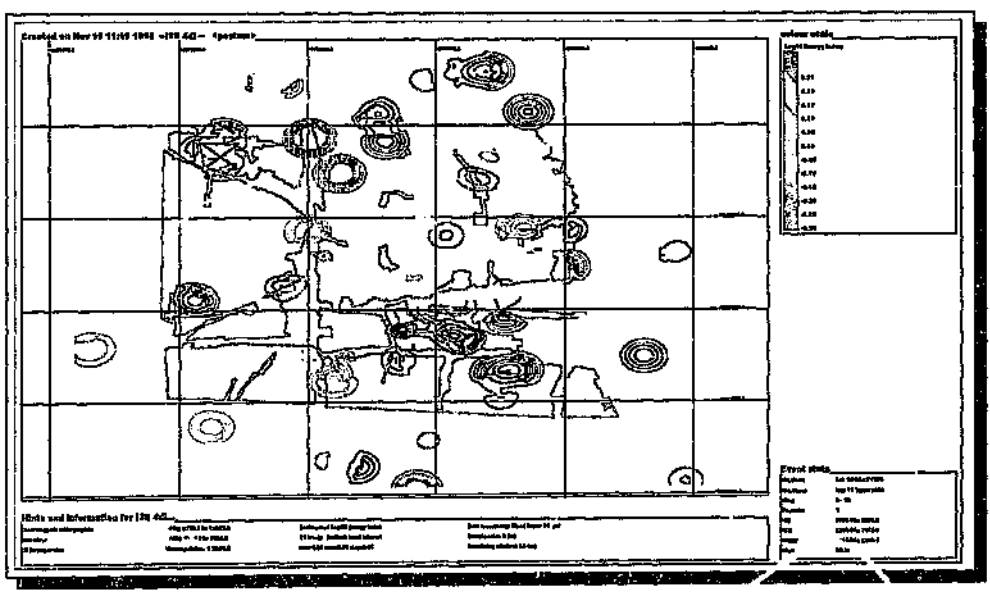

Fig. 4.125: Same as fig. 4.124; contours are of log(EI).

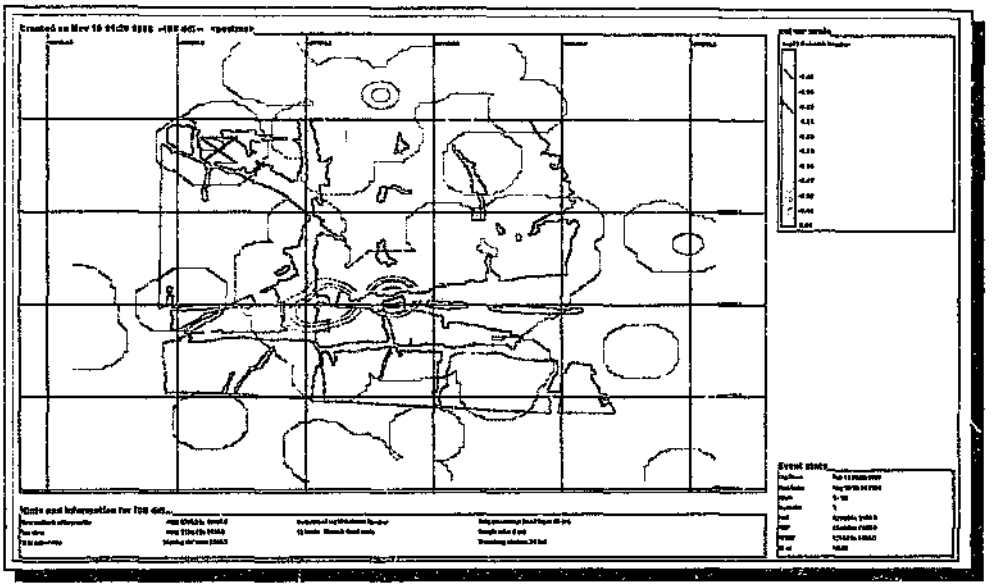

Fig. 4.126: Same as fig. 4.124; contours are of log(inv. Deborah n .).

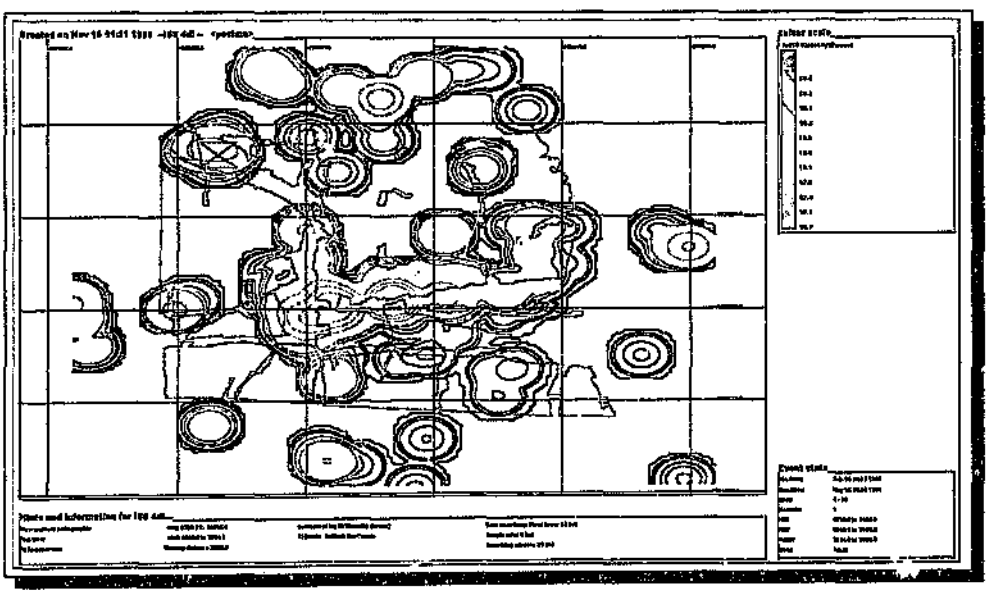

Fig. 4.127: Same as fig. 4.124; contours are of log(viscosity).

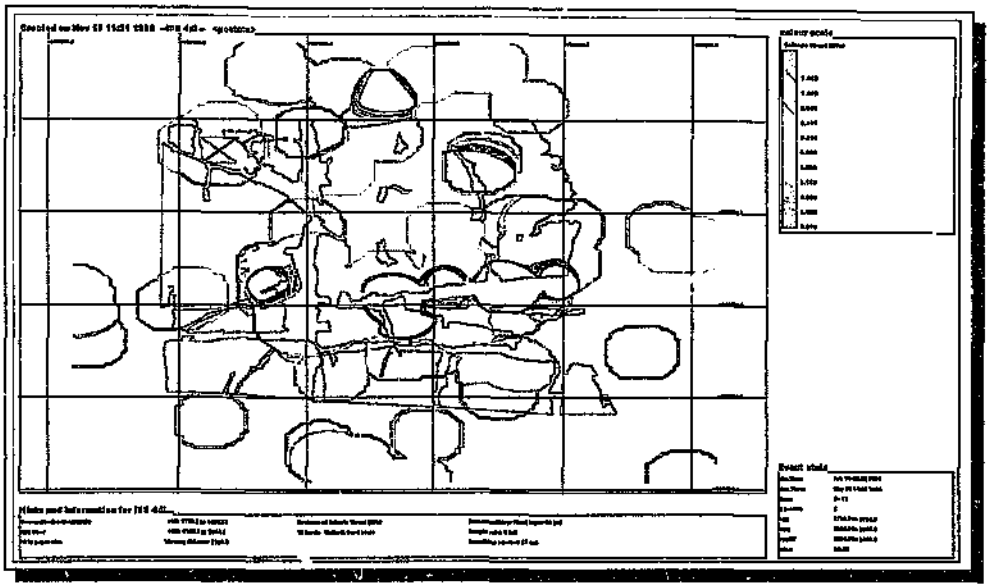

Fig. 4.128: Same as fig. 4.124; contours are of seismic stress.

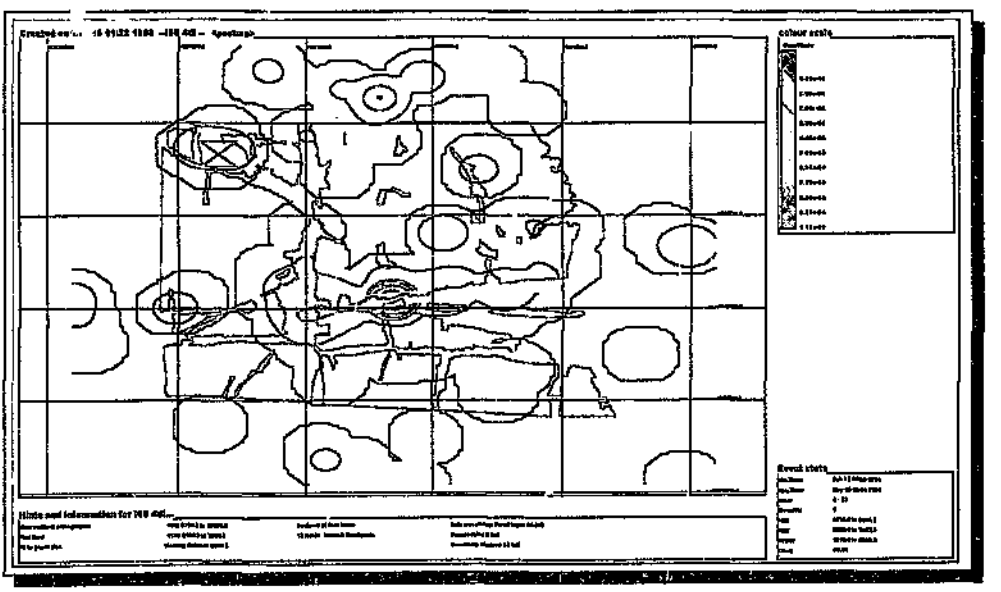

Fig. 4.129: Same as fig. 4.124; contours are of cumulative seismic strain. In a regional sense the prominent high on the Postma dyke draws attention away from the general locality of event 940513.

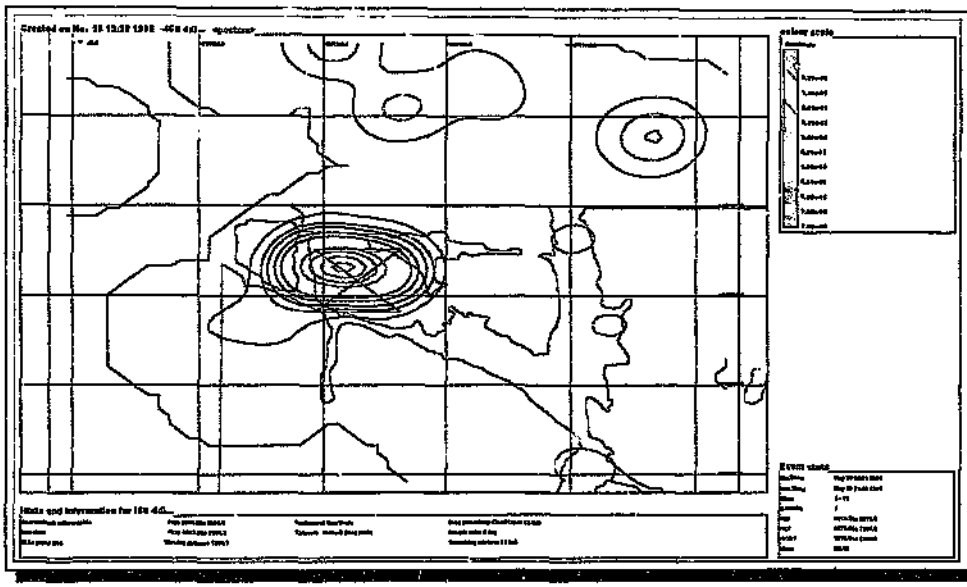

Fig. 4.130: A 'zoom-in' on the area of interest reveals a distinct percursory high in cumulative seismic strain which developed in a time interval of 13 months before event 940513.

APPENDIX F7

(a) Sections looking northwards along the plane of the Basson fault (fig. 4.132) and eastwards along the plane of the Postma dyke (fig. 4.133), with events represented by seismic a- ent volume in relation to the broken 'planes' of the Basal Reef.

(b) Time-history and contour plots used in the analysis of events 940627a, 940627b and 940627c to identify precursors (figs. 4.134 - 4.168); Section 4.2.7, Chapter 4.

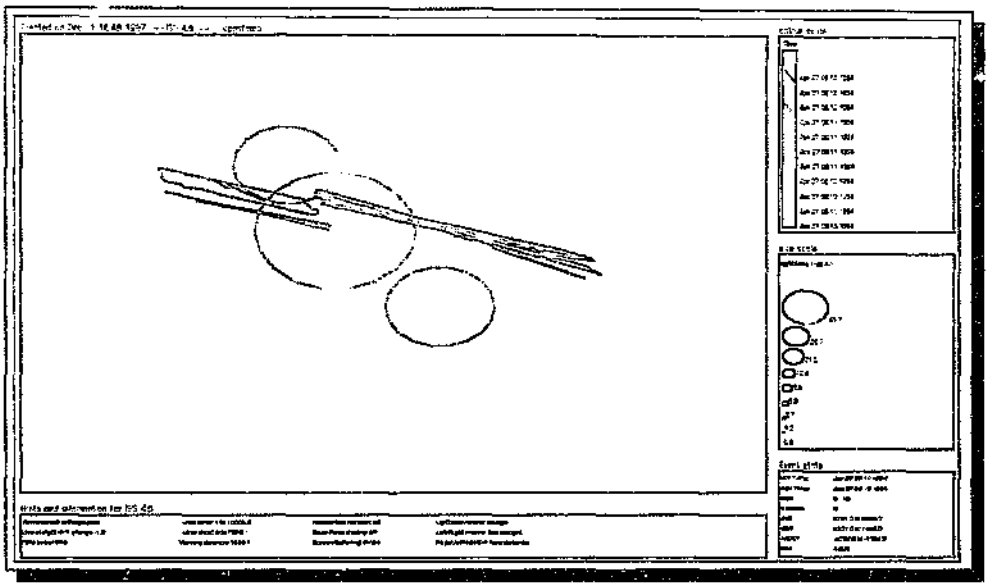

Fig. 4.132: Section looking northwards, along the plane of the Basson fault, onto the Postma dyke, with events 940627a, 940627b and 940627c represented by seismic apparent volume in relation to the broken 'planes' of the Basal reef. For vertical scale consider the dip extent of the Postma dyke model (340 m).

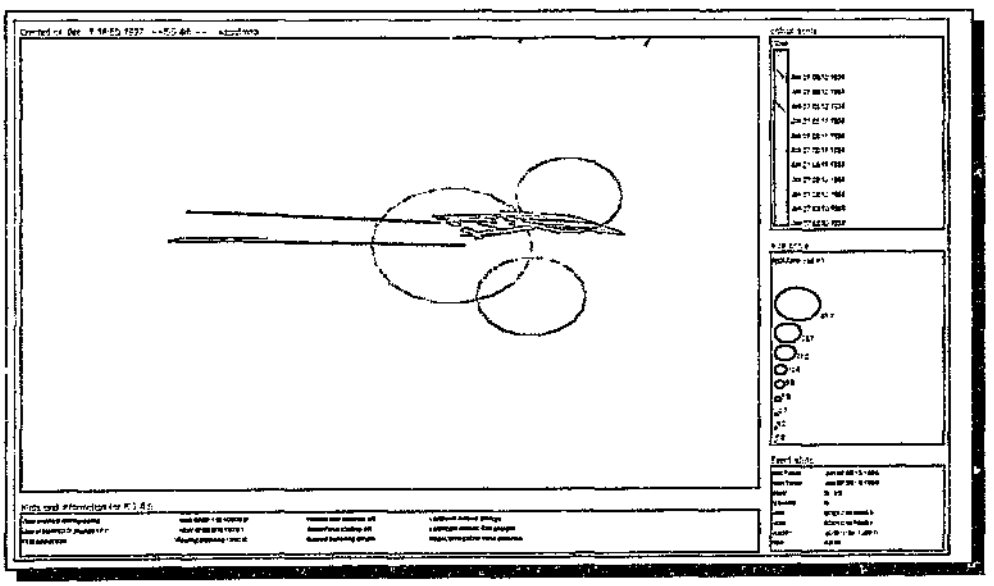

Fig. 4.133: Same as above, but looking eastwards along the plane of the Postma dyke, onto the Basson fault, downdip along the Basal reef. For vertical scale consider the dip extent of the Basson fault model (280 m).

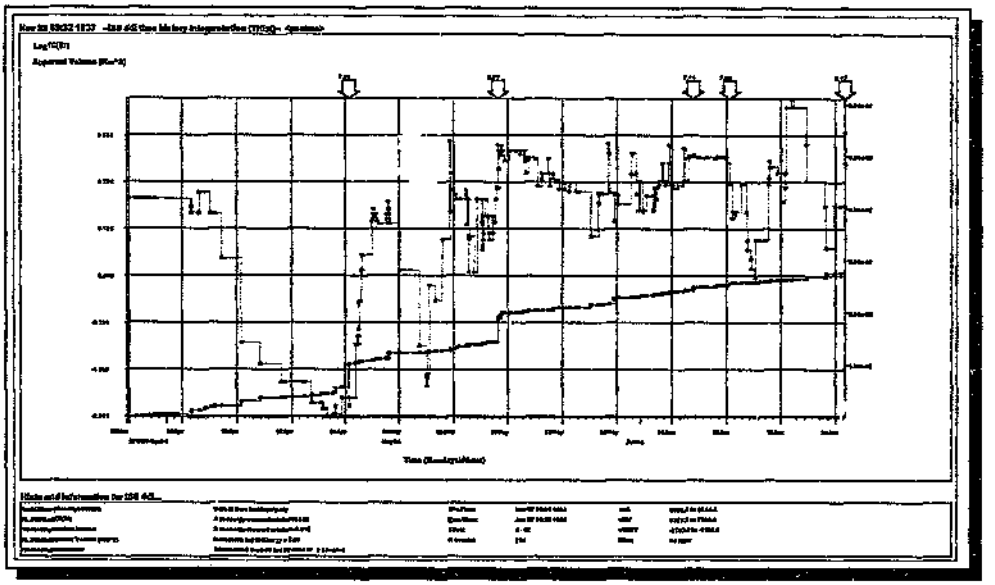

Fig. 4.134: Time-history of cumulative apparent volume and moving median log(EI), using a moving data window of 8 samples and/or 5 days, for seismicity recorded in the time period 27/3/94 to 27/6/94. The last arrow in time refers to event 940627a.

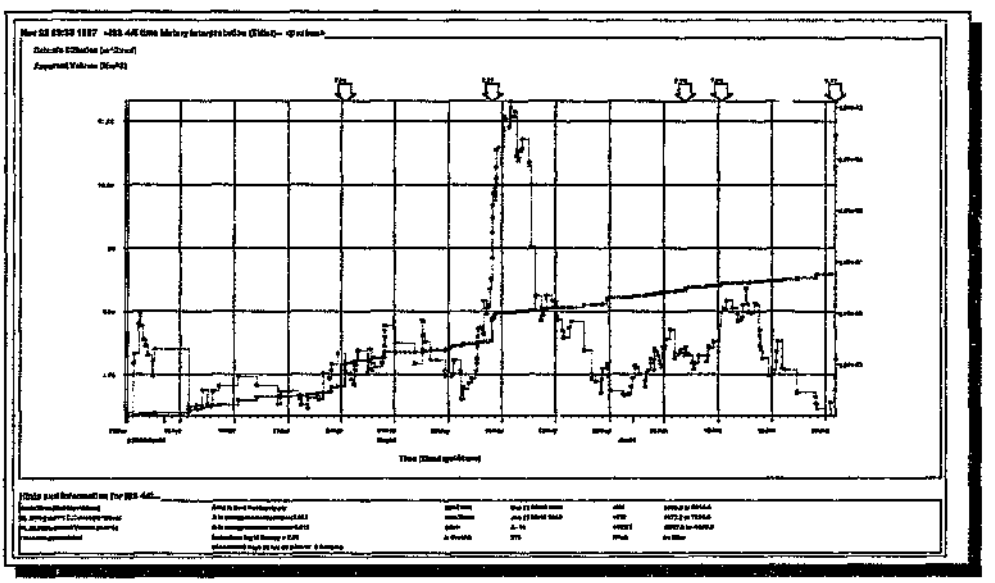

Fig. 4.135: Same as fig. 4.134, showing variation of seismic diffusion.

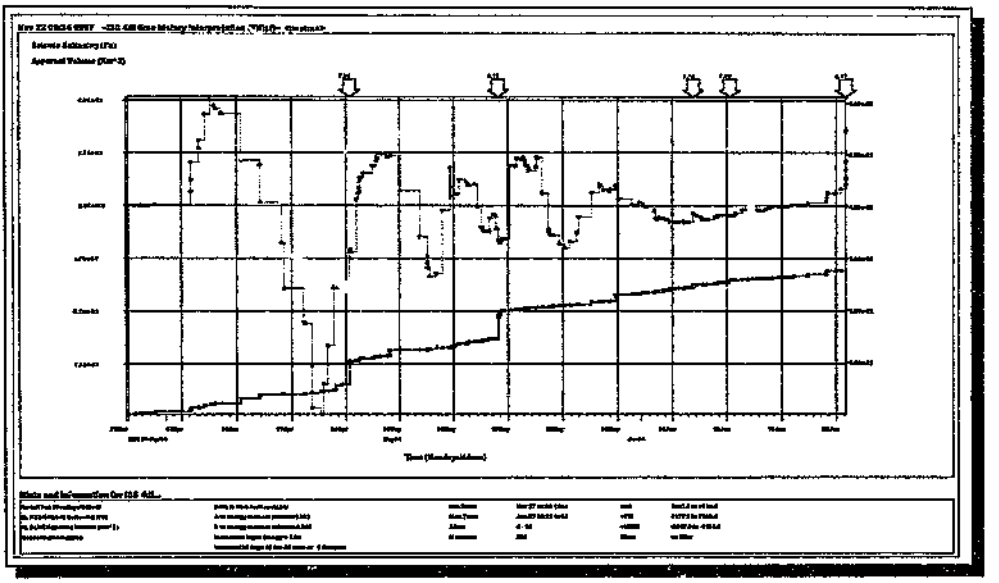

Fig. 4.136: Same as fig. 4.134, showing variation of seismic softening.

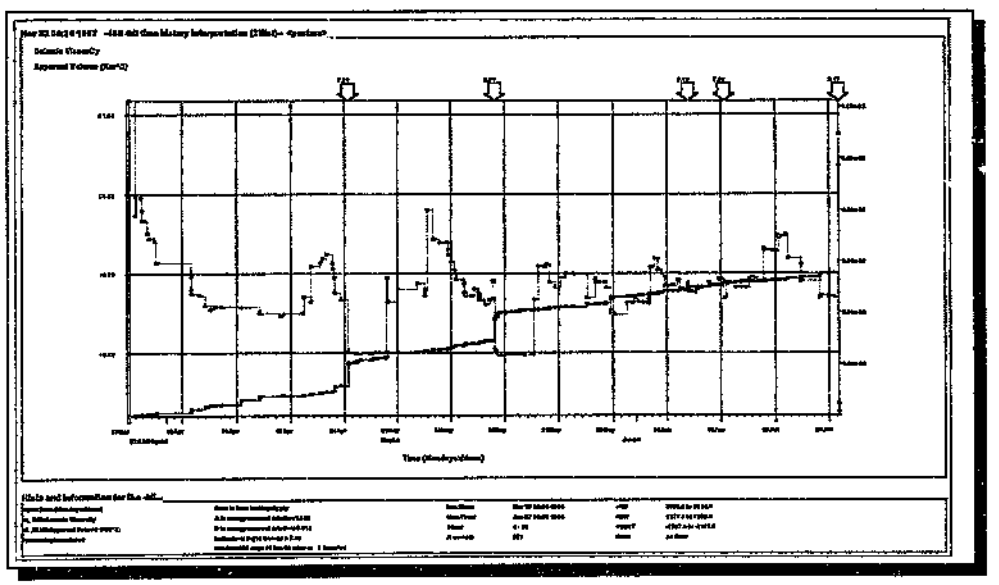

Fig. 4.137: Same as fig. 4.134, showing variation of seismic viscosity.

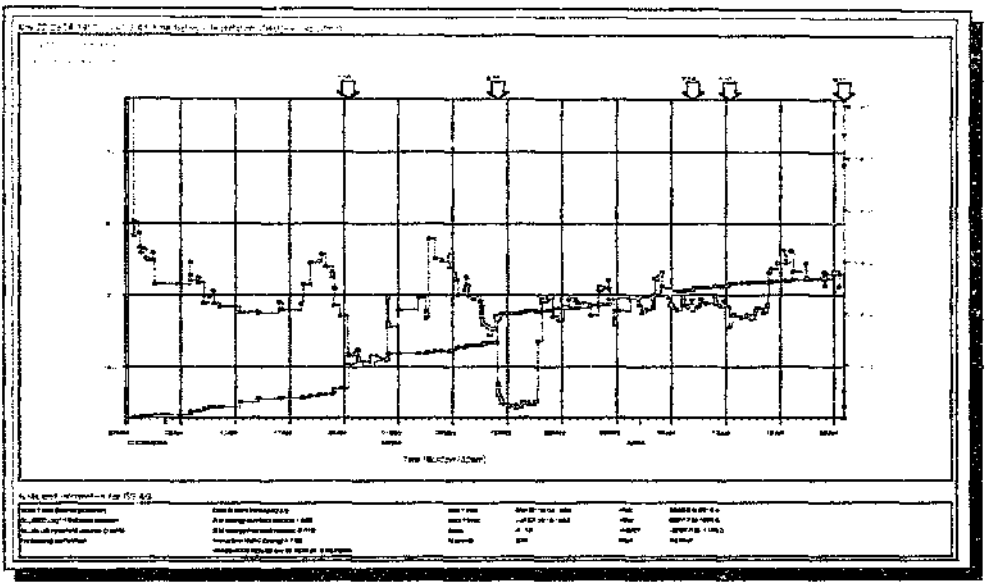

Fig. 4.138: Same as fig. 4.134, showing variation in log(seismic Schmidt number).

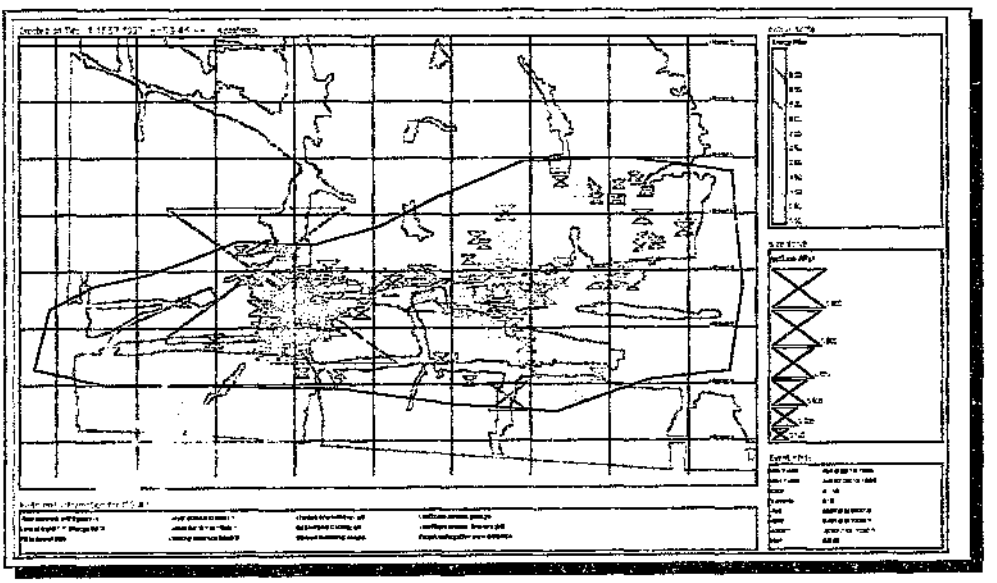

Fig. 4.139: Distribution of events in the time period 5/4/94 to 27/6/94 within the modified polygon to select only that seismicity closest to the Postma dyke.

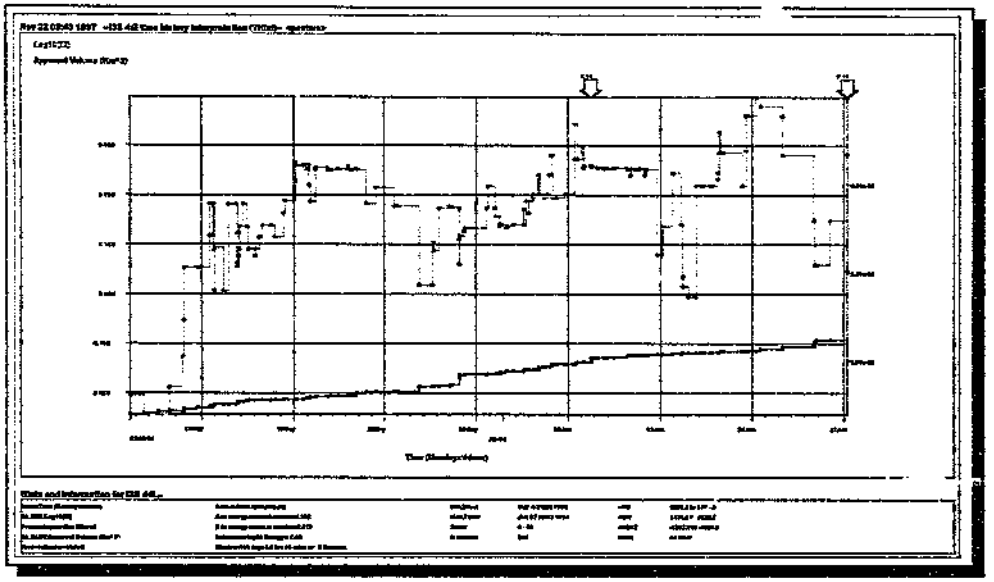

Fig. 4.140: Time-history of cumulative apparent volume and moving median log(EI), based on the seismicity selected within the modified polygon shown in fig. 4.139. The seismicity is represented in the time period 3/5/94 to 27/6/94. The last arrow in time refers to event 940627a.

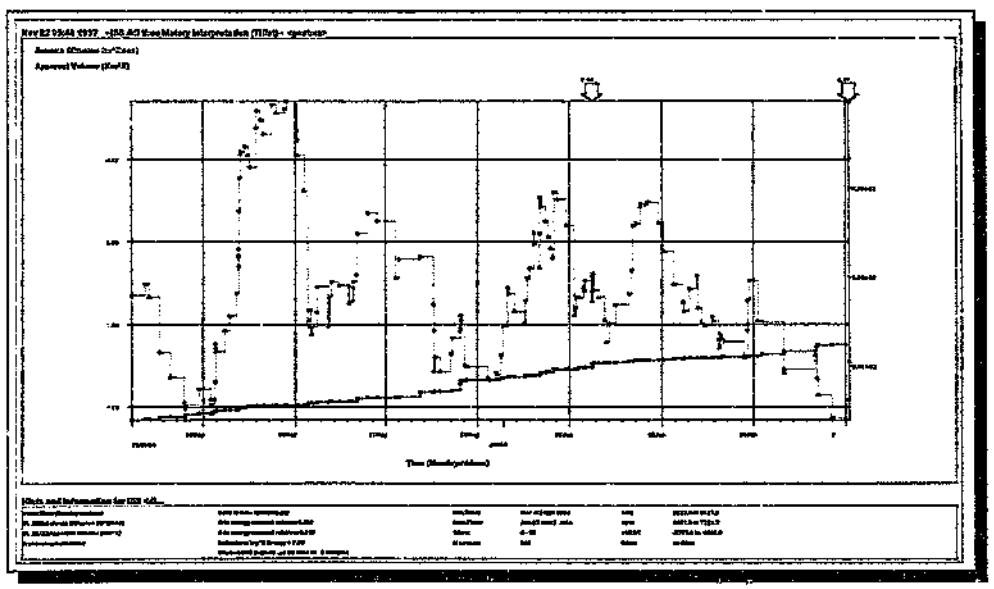

Fig. 4.141: Same as fig. 4.140, showing variation of seismic diffusion.

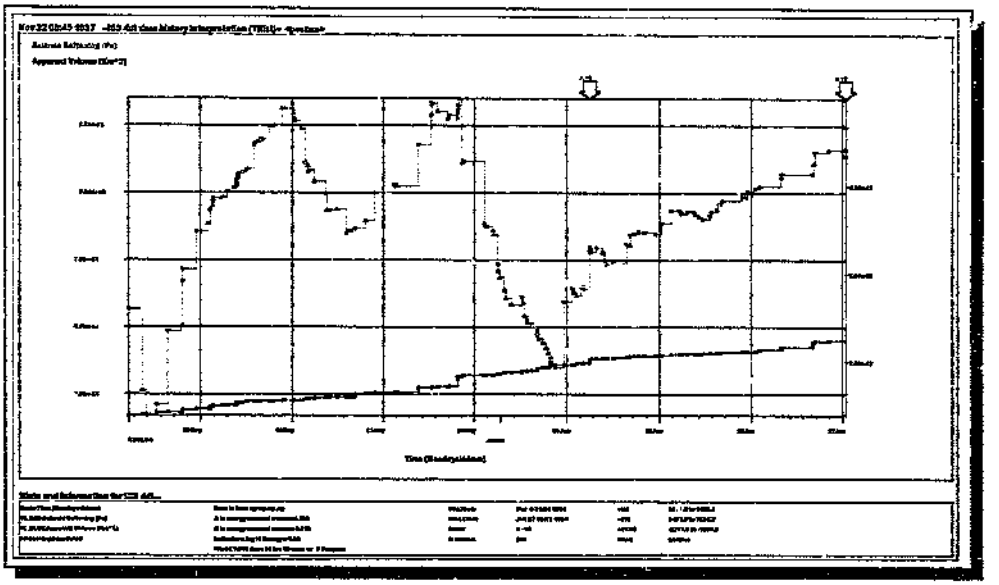

Fig. 4.142: Same as fig. 4.140, showing variation of seismic diffusion.

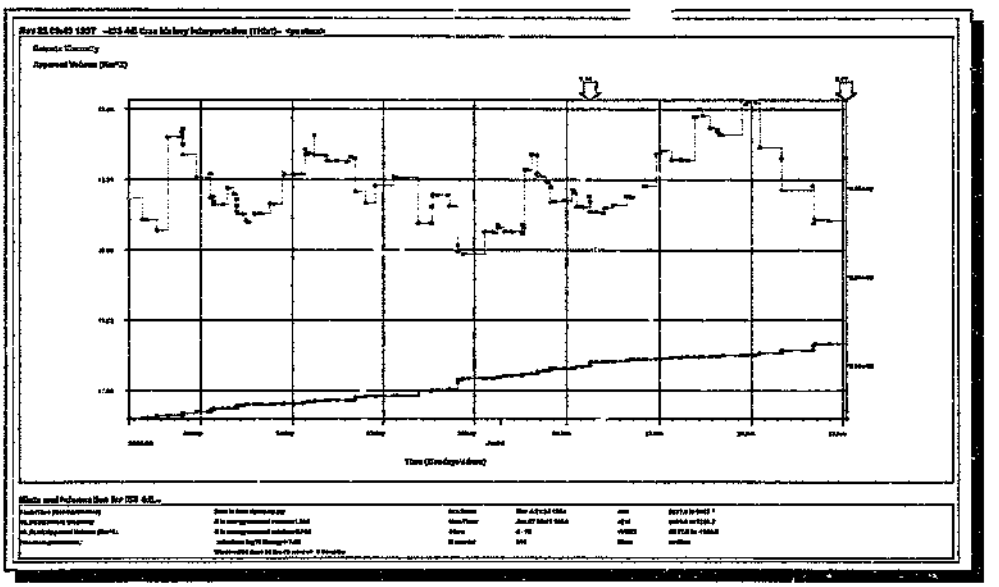

Fig. 4.143: Same as fig. 4.140, showing variation of seismic viscosity.

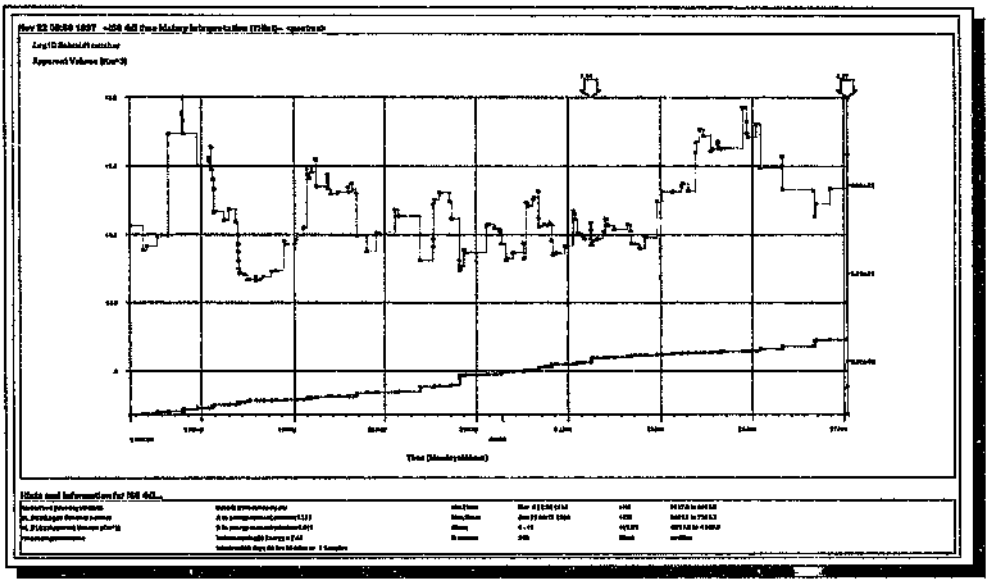

Fig. 4.144: Same as fig. 4.140, showing variation in log(seismic Schmidt no.).

Contour plots of those seismic parameters under investigation relating to the seismicity recorded 12 months before (but excluding) events 940627a, 940627b and 940627c (figs. 4.145 - 4.150).

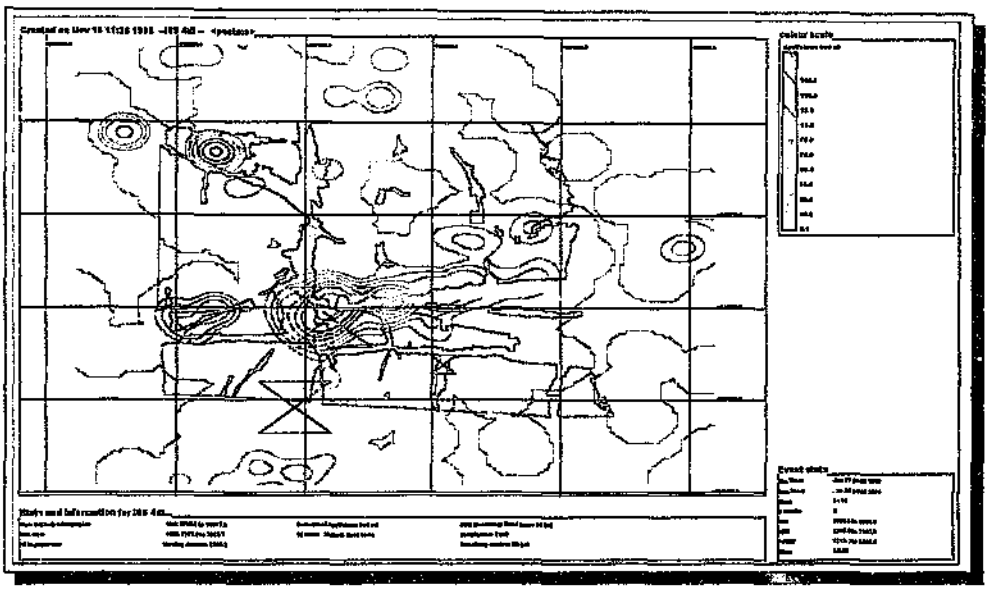

Fig. 4.145: Contours of apparent volume using seismicity recorded in the time period 27/6/93 to 26/6/94 (12 months leading up to, but excluding, events 940627a, 940627b and 940627c, the locations of which are indicated by the 'hourglass' symbols).

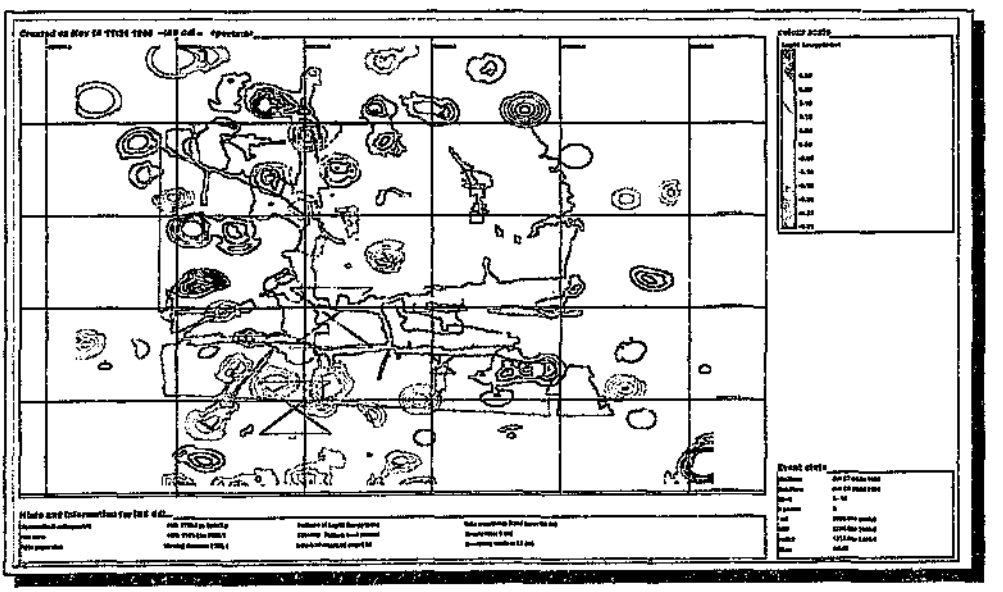

Fig. 4.146: Same as fig. 4.145, but contours are of log(EI).

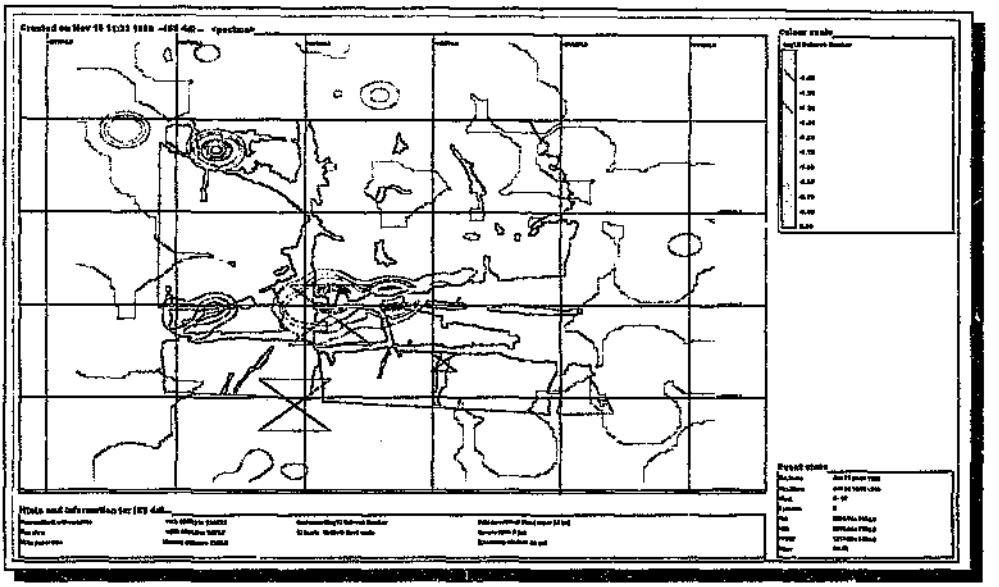

Fig. 4.147: Same as fig. 4.145, but contours are of log(inv. Deborah n[illegible]).

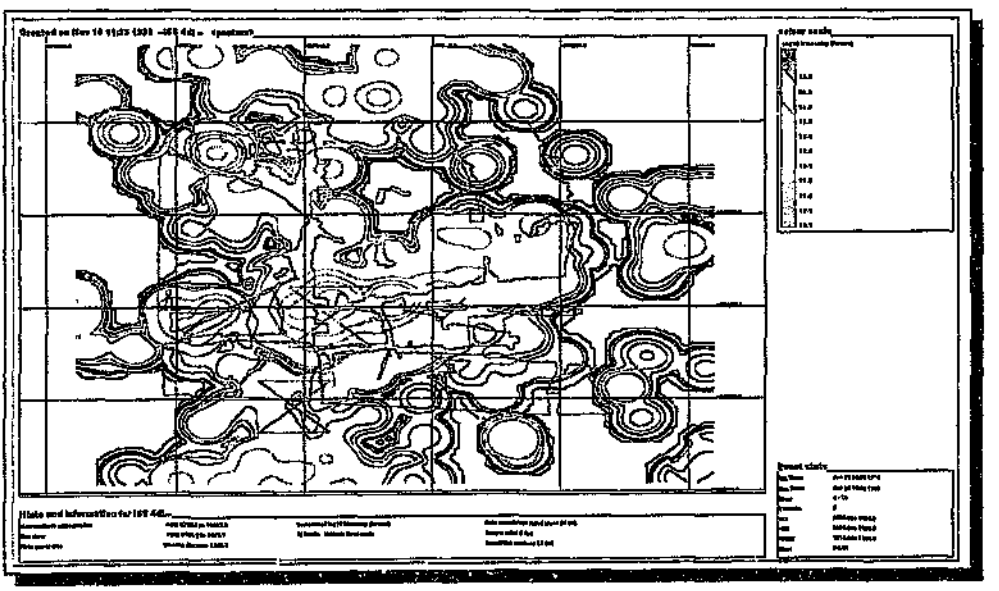

Fig. 4.148: Same as fig. 4.145; contours are of log(viscosity).

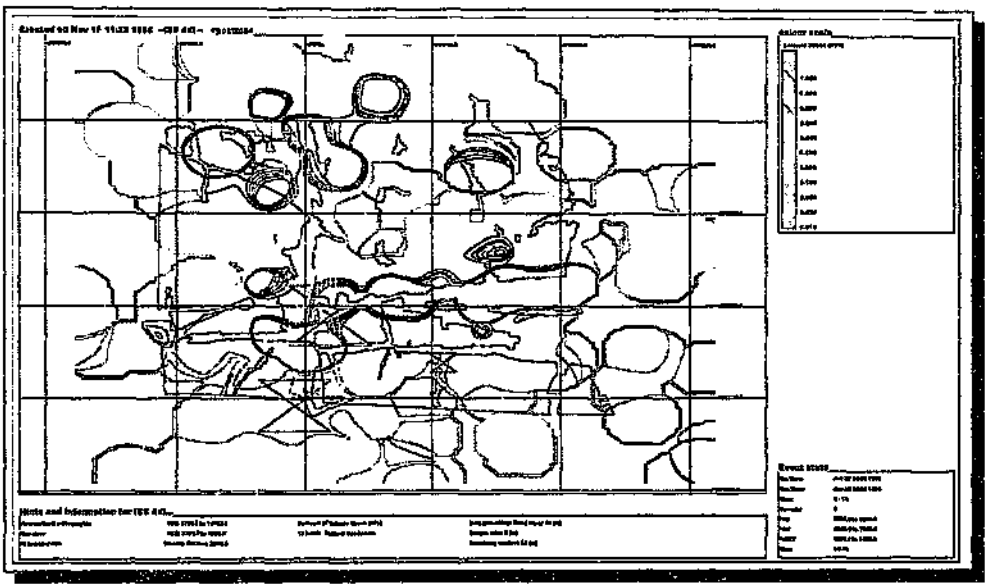

Fig. 4.149: Same as fig. 4.145; contours are of seismic stress.

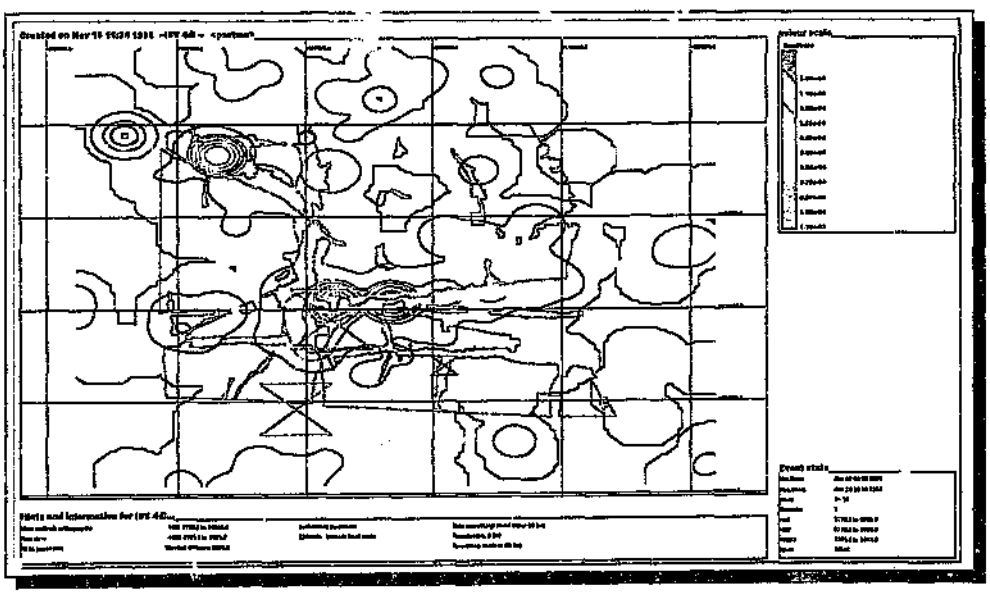

Fig. 4.150: Same as fig. 4.145, contours are of cumulative seismic strain.

Contour plots of those seismic parameters under investigation relating to the seismicity recorded 6 months before (but excluding) events 940627a, 940627b and 940627c (figs. 4.151 - 4.156).

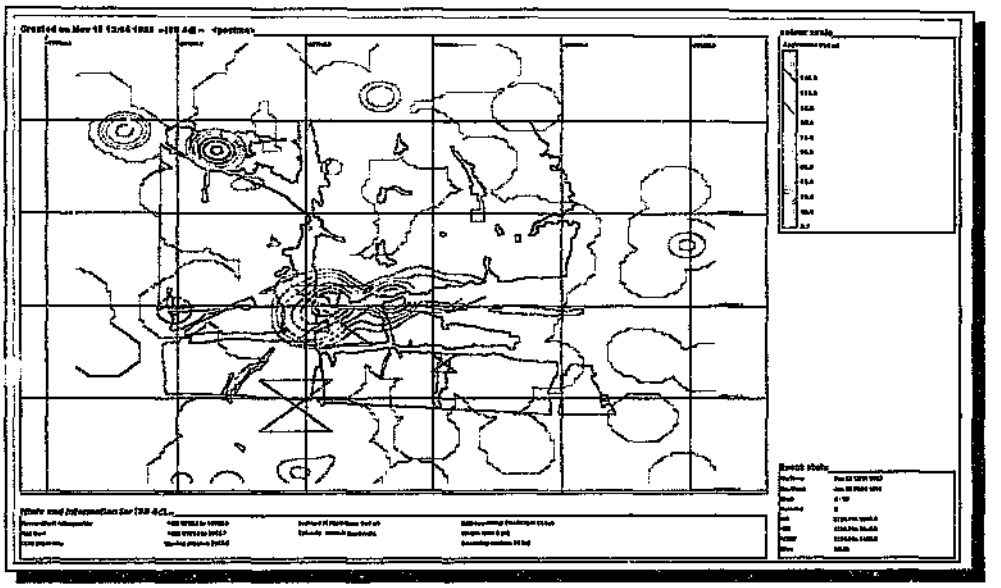

Fig. 4.151: Contours of apparent volume using seismicity recorded in the time period 27/12/93 to 26/6/94 (six months leading up to, but excluding, events 940627a, 940627b and 940627c, the locations of which are indicated by the 'hourglass' symbols).

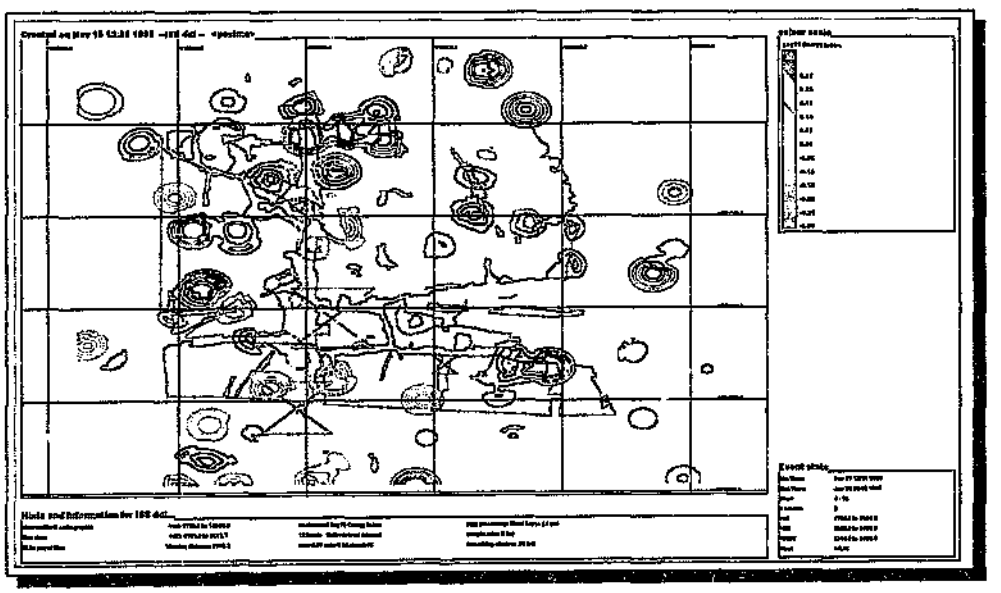

Fig. 4.152: Same as fig. 4.151; contours are of log(EI).

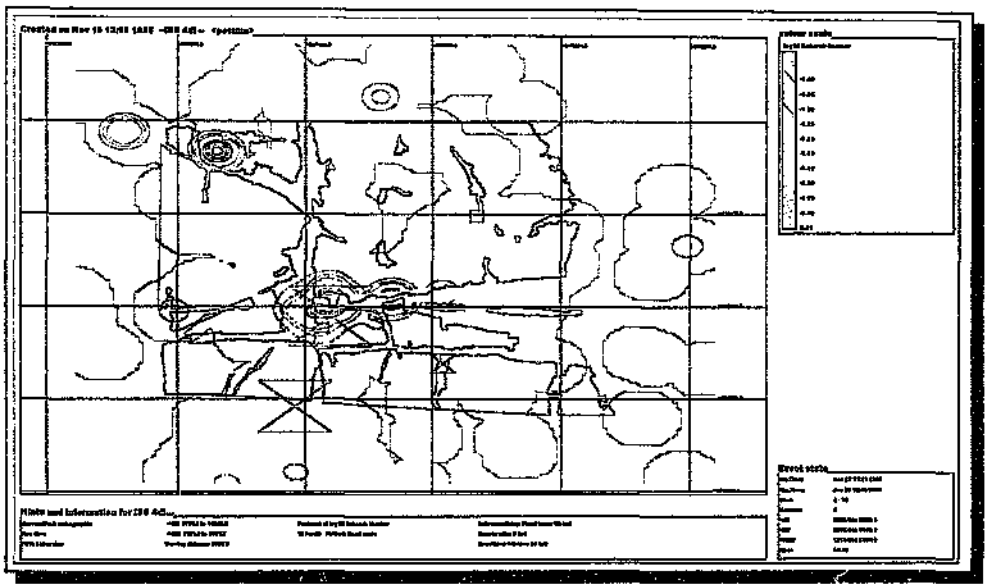

Fig. 4.153: Same as fig. 4.151; contours are of log(inv. Deborah no.).

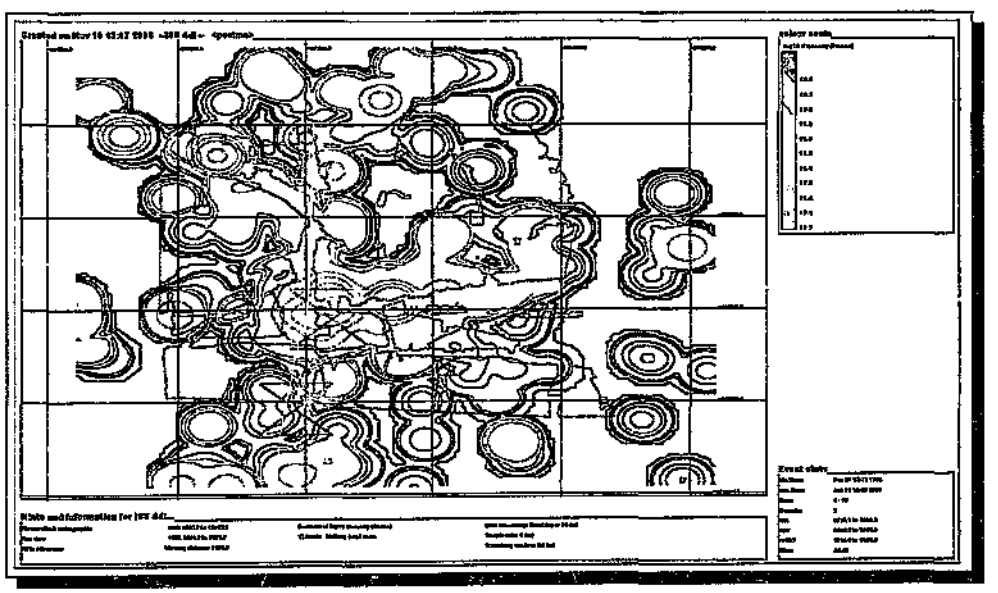

Fig. 4.154: Same as fig. 4.151; contours are of log(viscosity).

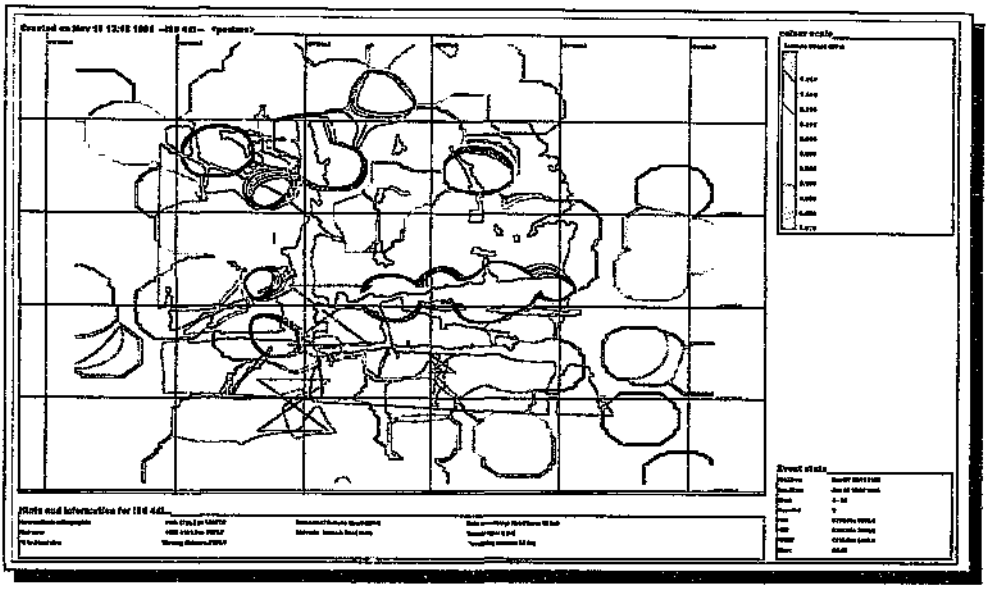

Fig. 4.155: Same as fig. 4.151; contours are of seismic stress.

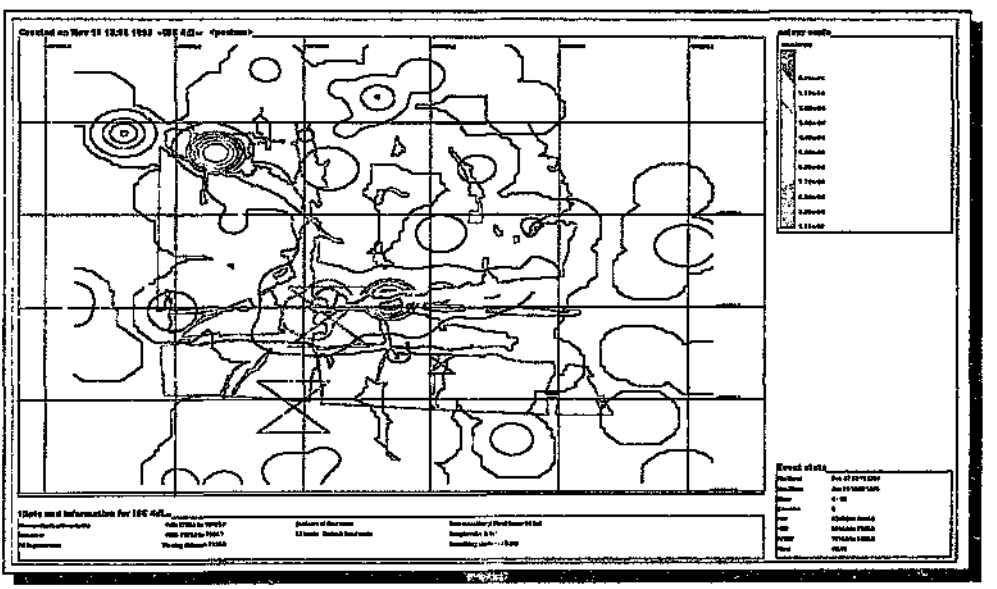

Fig. 4.156: Same as fig. 4.151; contours are of cumulative seismic strain.

Contour plots of those seismic parameters under investigation relating to the seismicity recorded 3 months before (but excluding) events 940627a, 940627b and 940627c (figs. 4.157 - 4.162).

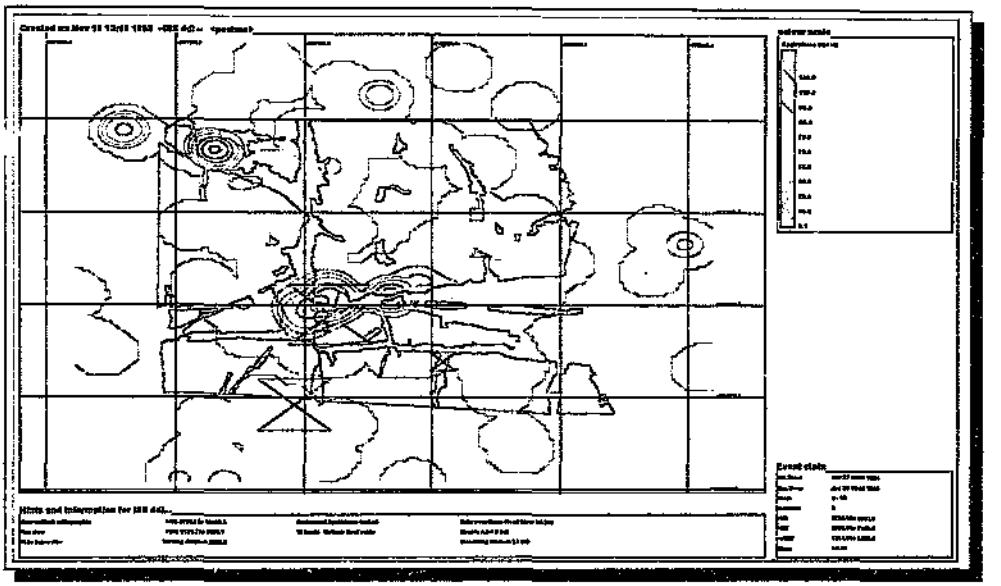

Fig. 4.157: Contours of apparent volume using seismicity recorded in the time period 27/3/94 to 26/6/94 (three months leading up to, but excluding, events 940627a, 940627b and 940627c, the locations of which are indicated by the 'hourglass' symbols).

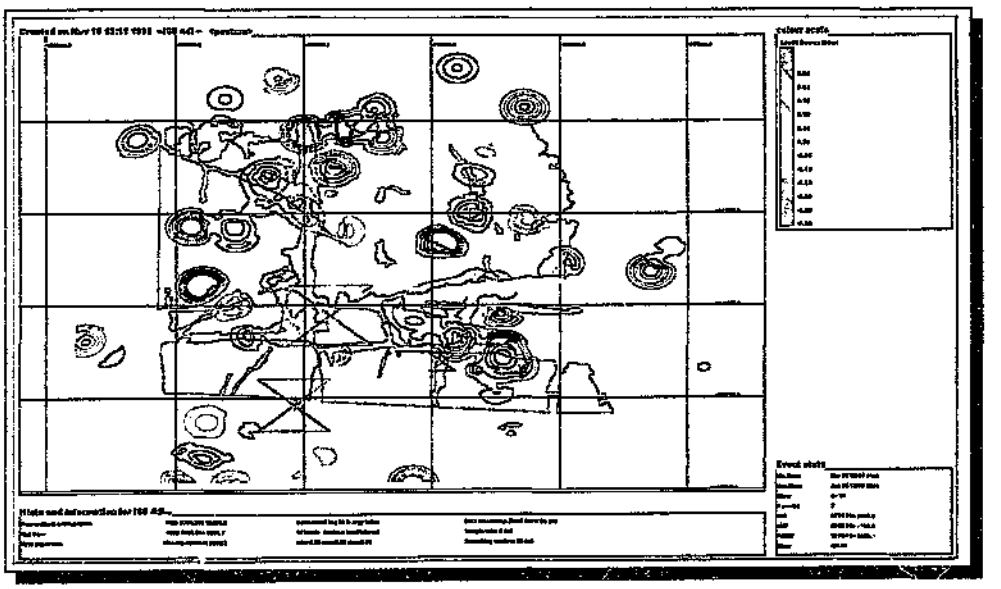

Fig. 4.158: Same as fig. 4.157; contours are of log(EI).

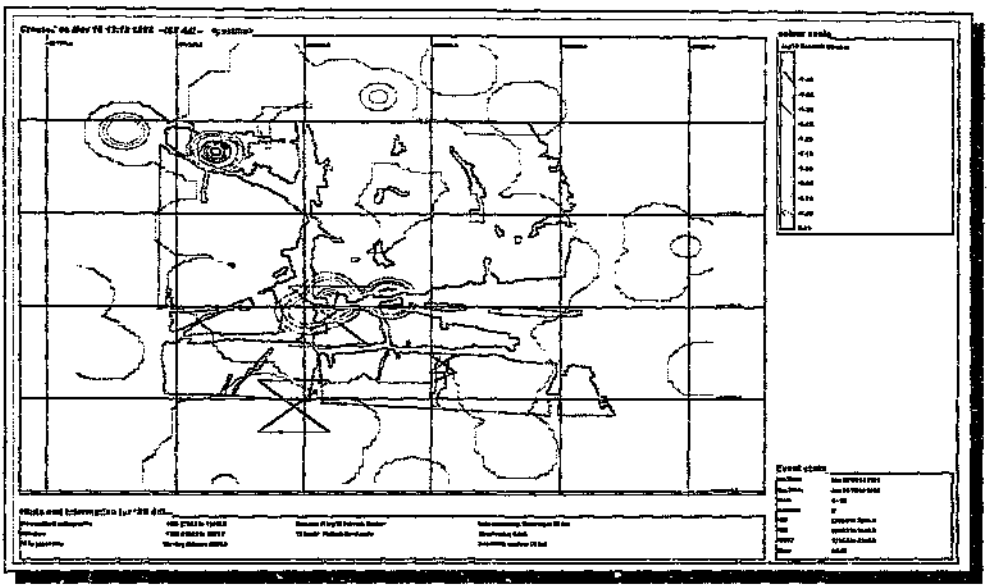

Fig. 4.159: Same as fig. 4.157; contours are of log(inv. Deborah no.).

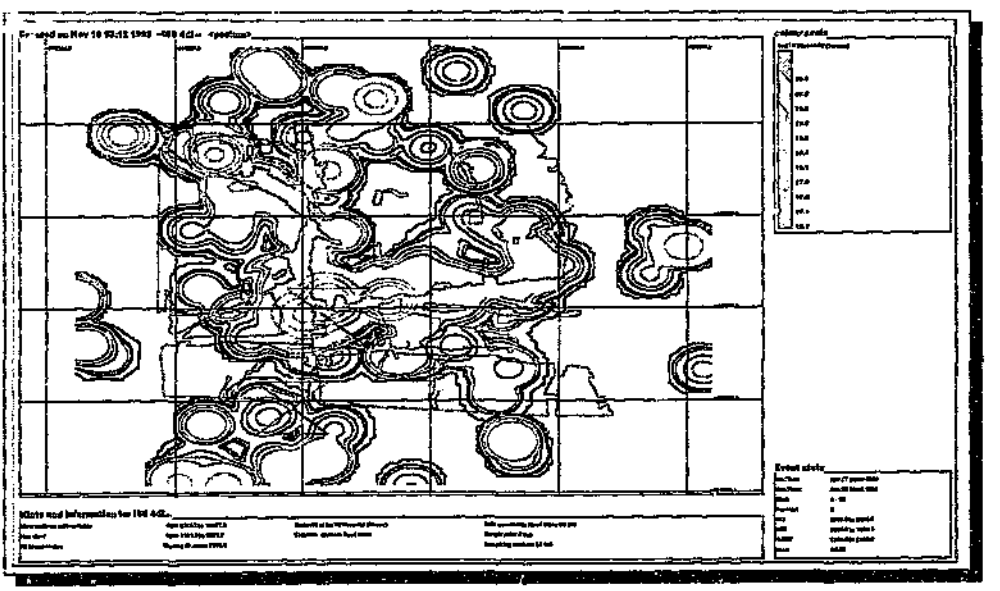

Fig. 4.160: Same as fig. 4.157; contours are of log(viscosity).

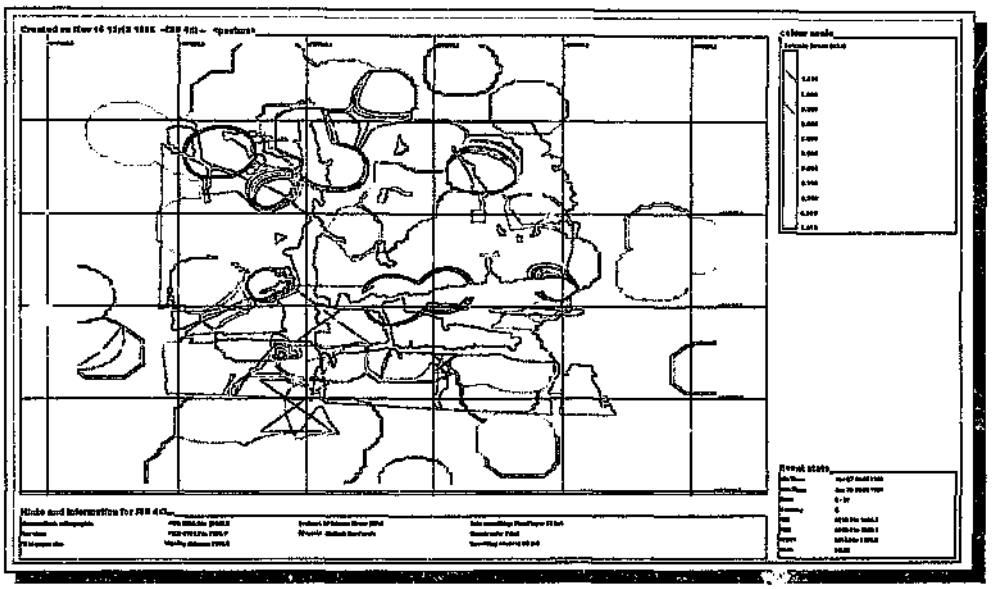

Fig. 4.161: Same as fig. 4.157; contours are of seismic stress.

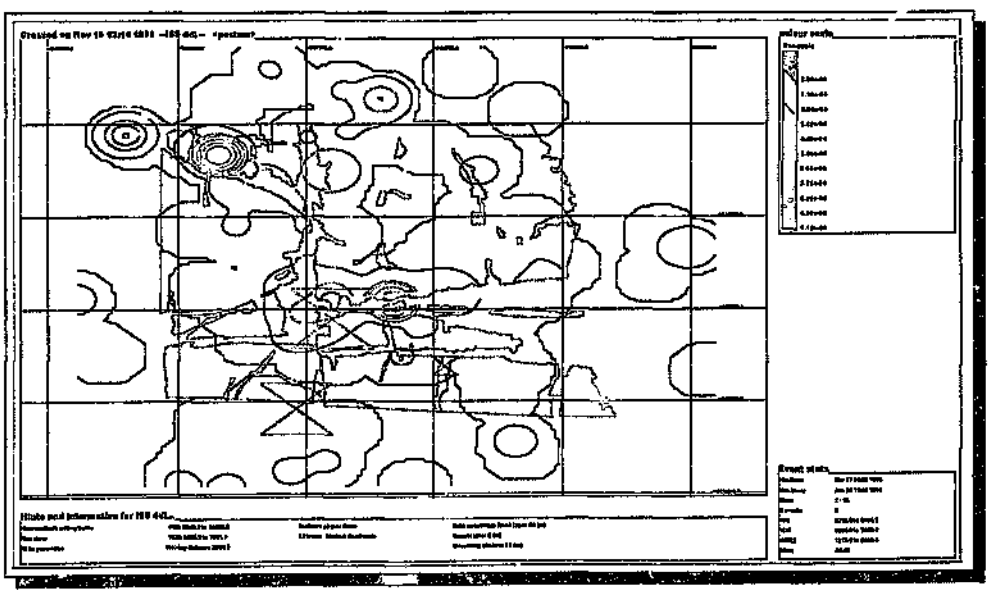

Fig. 4.162: Same as fig. 4.157; contours are of cumulative seismic strain.

Contour plots of those seismic parameters under investigation relating to the seismicity recorded one month before (but excluding) events 940627a, 940627b and 940627c (figs. 4.163 - 4.168).

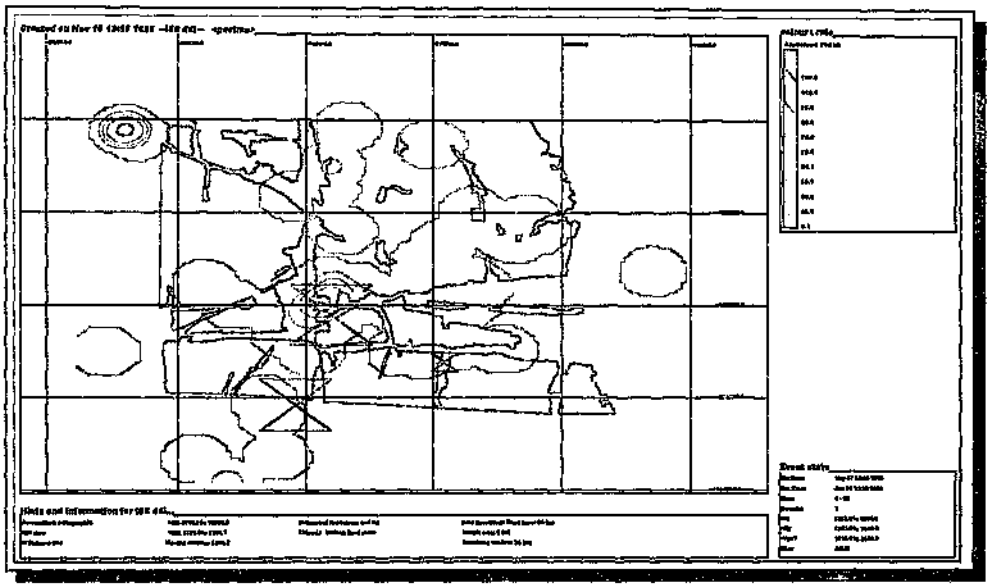

Fig. 4.163: Contours of apparent volume using seismicity recorded in the time period 27/5/94 to 26/6/94 (one month leading up to, but excluding events 940627a, 940627b and 940627c, the locations of which are indicated by the 'hourglass' symbols).

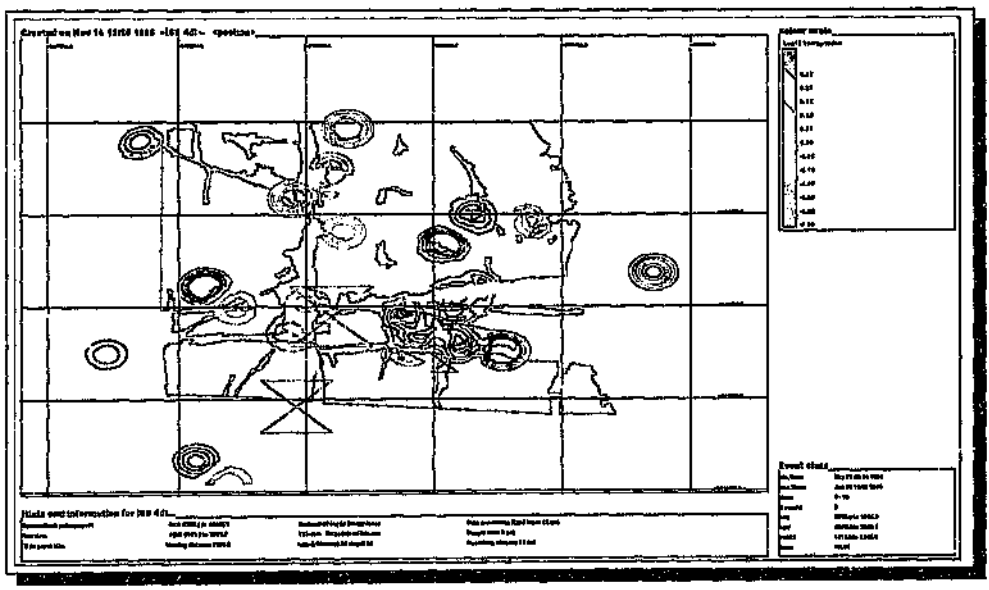

Fig. 4.164: Same as fig. 4.163; contours are of log(EI).

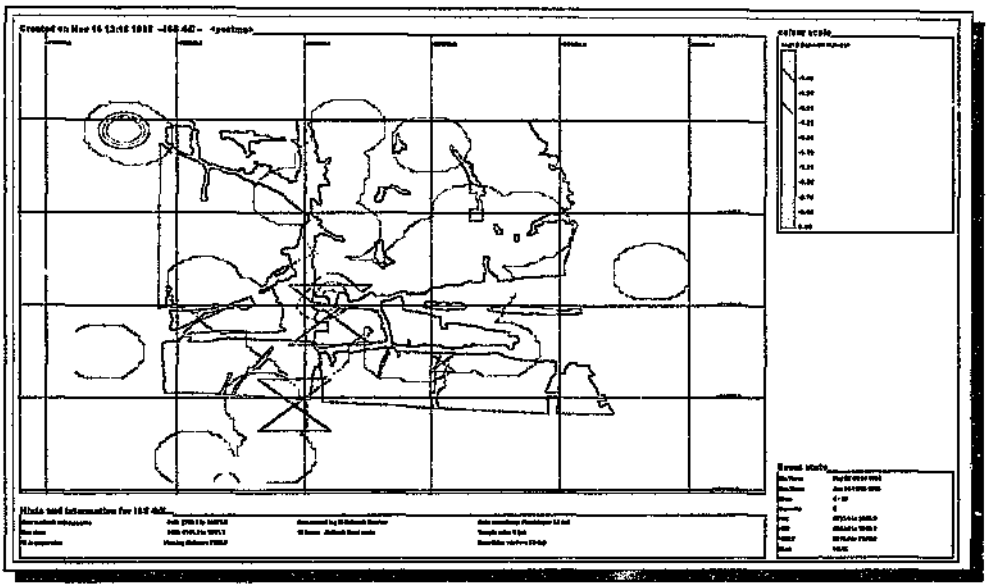

Fig. 4.165: Same as fig. 4.163; contours are of log(inv. Deborah no.).

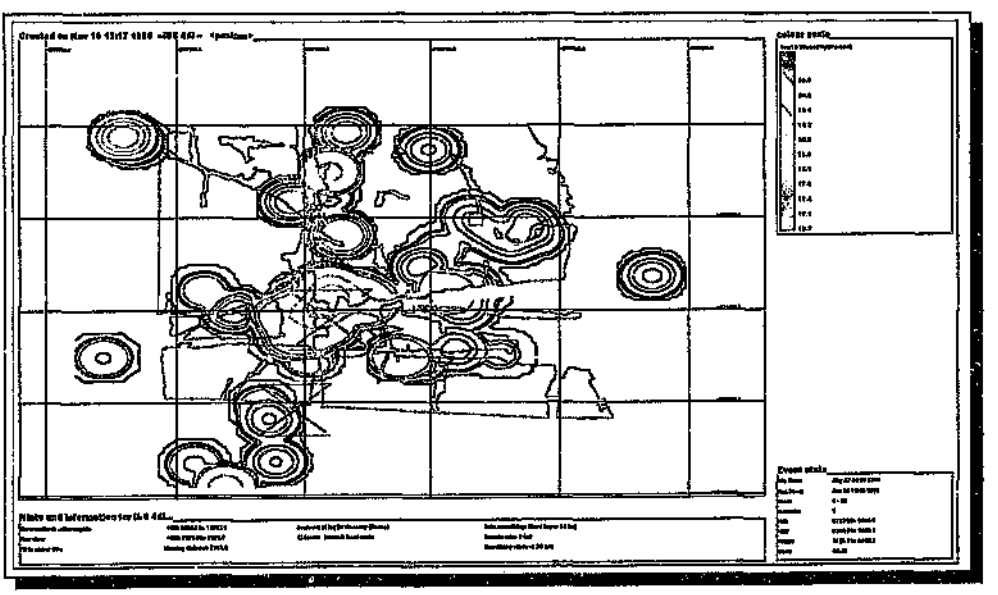

Fig. 4.166: Same as fig. 4.163; contours are of log(viscosity).

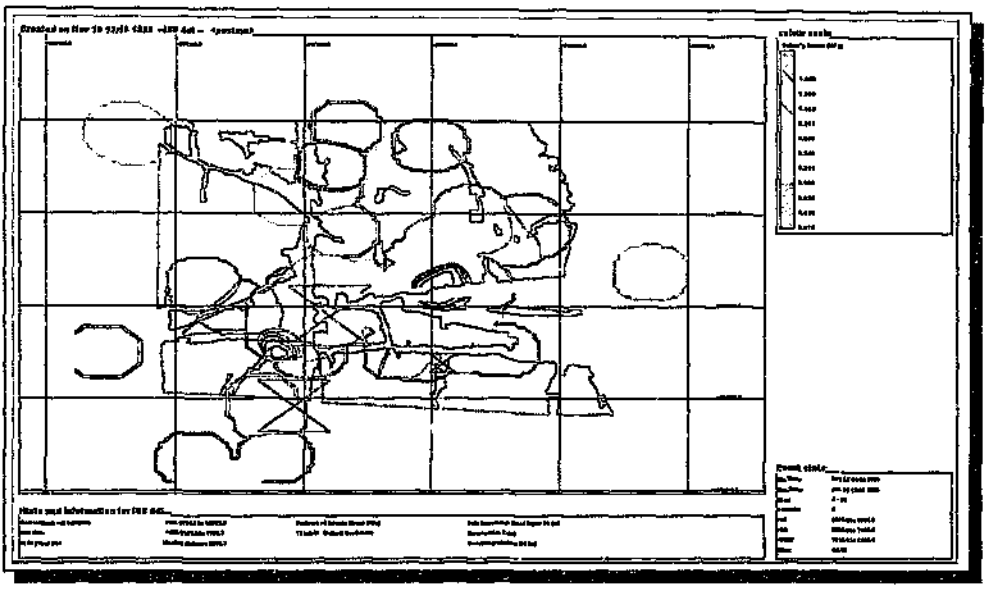

Fig. 4.167: Same as fig. 4.163; contours are of seismic stress.

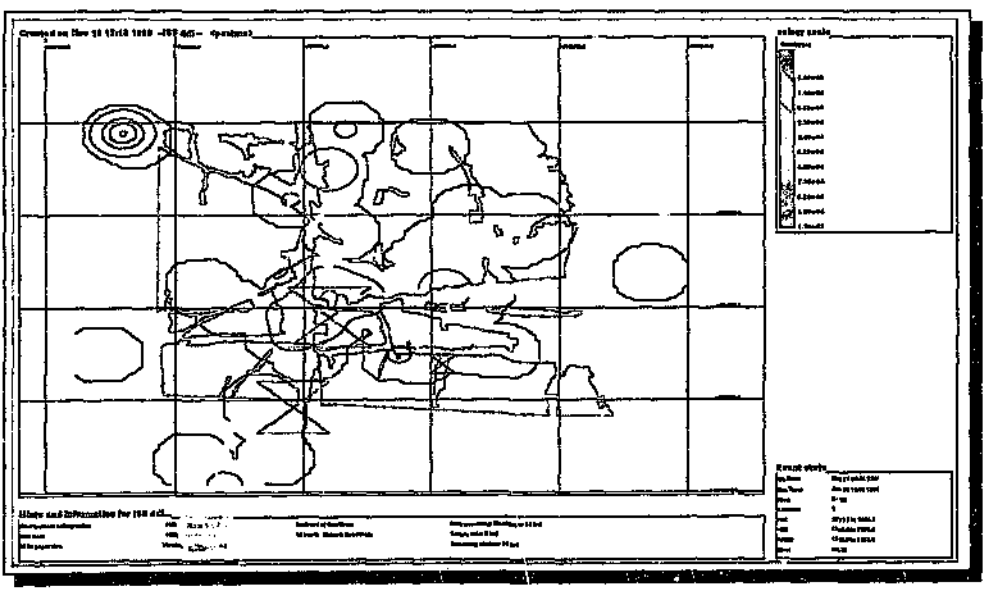

Fig. 4.168: Same as fig. 4.163; contours are of cumulative seismic strain.

APPENDIX G

Sensitivity of source parameter calculations to the length of time windows used (figs. 4.169 - 4.198); Section 4.2.7, Chapter 4.

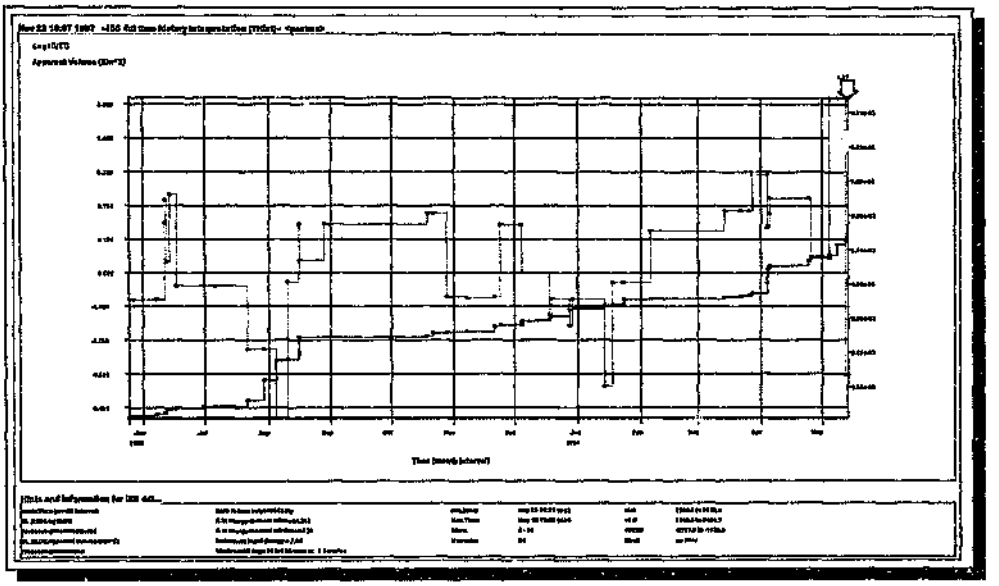

Fig. 4.169: Sensitivity of median log(EI) to a moving window of 5 days and/or 3 samples of data (see text); the time-history of cumulative apparent volume is used as a reference in each subsequent case (figs. 4.170 to 4.177; the time period of seismicity is held constant from 25/5/93 to 13/5/94). The arrow refers to event 940513.

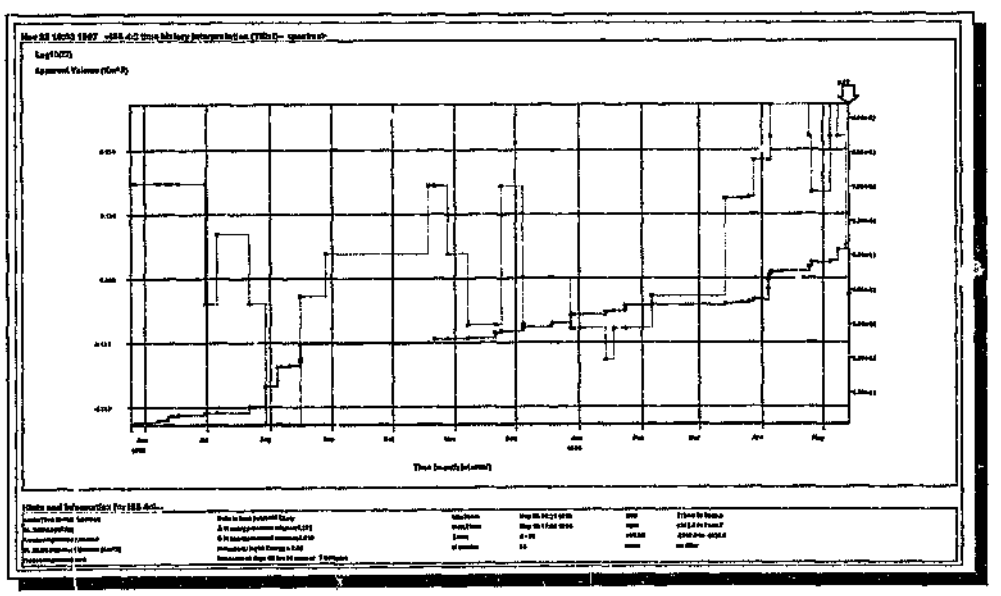

Fig. 4.170: Same as above, but using a moving window of 5 days and/or 7 samples of data.

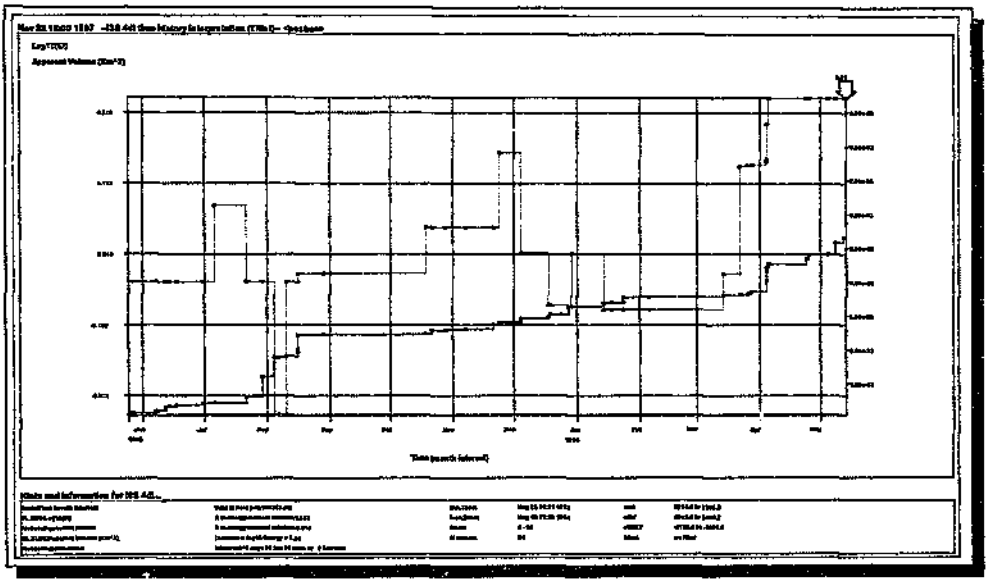

Fig. 4.171: Same as fig. 4.169, but using a moving window of 5 days and/or 9 samples of data.

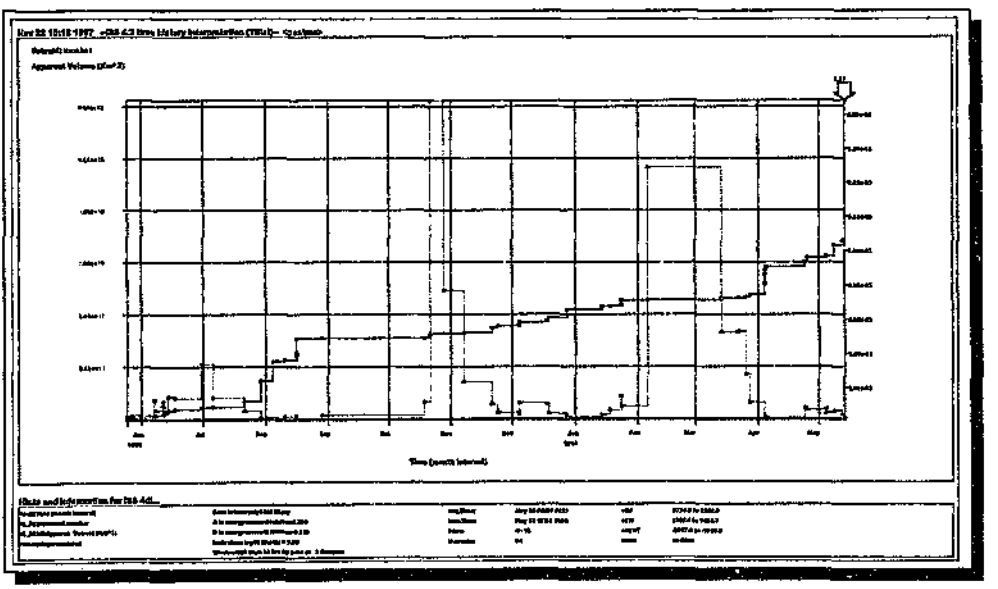

Fig. 4.172: Sensitivity of median seismic Schmidt number to a moving window of 5 days and/or 3 samples of data.

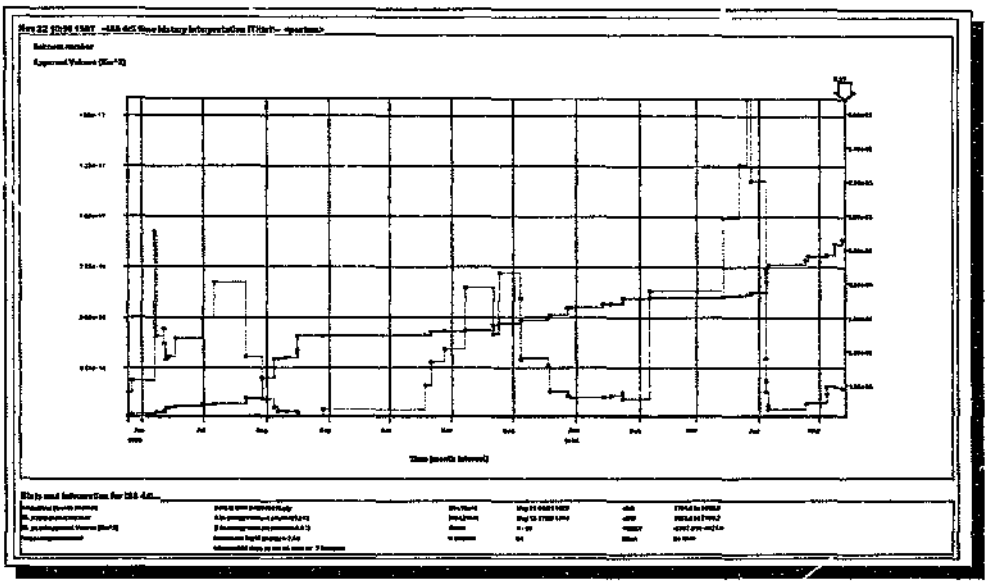

Fig. 4.173: Same as fig. 4.172, but with moving window of 5 days and/or 7 samples of data.

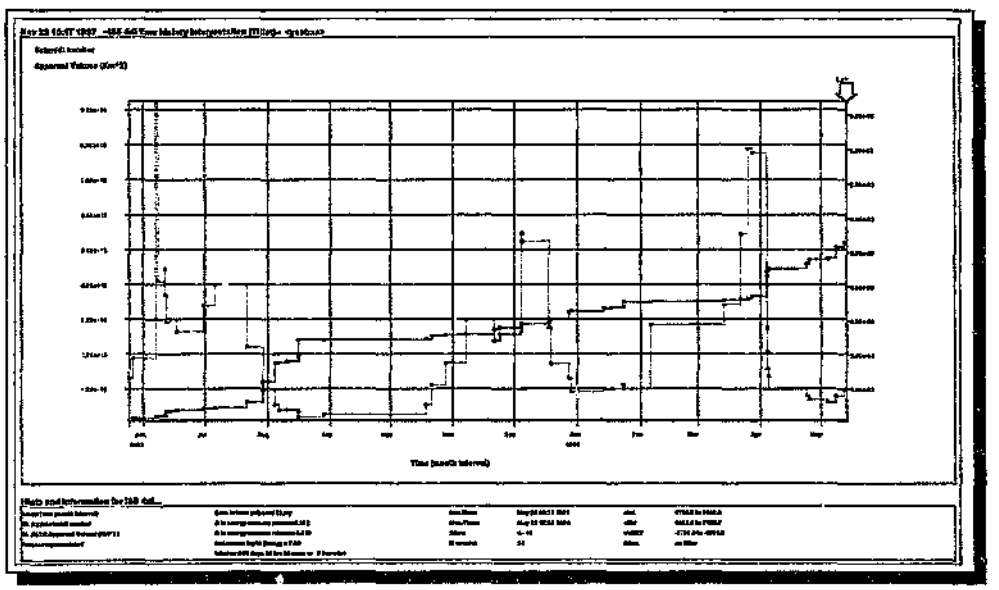

Fig. 4.174: Same as fig. 4.172, but with a moving window of 5days and/or 9 samples of data.

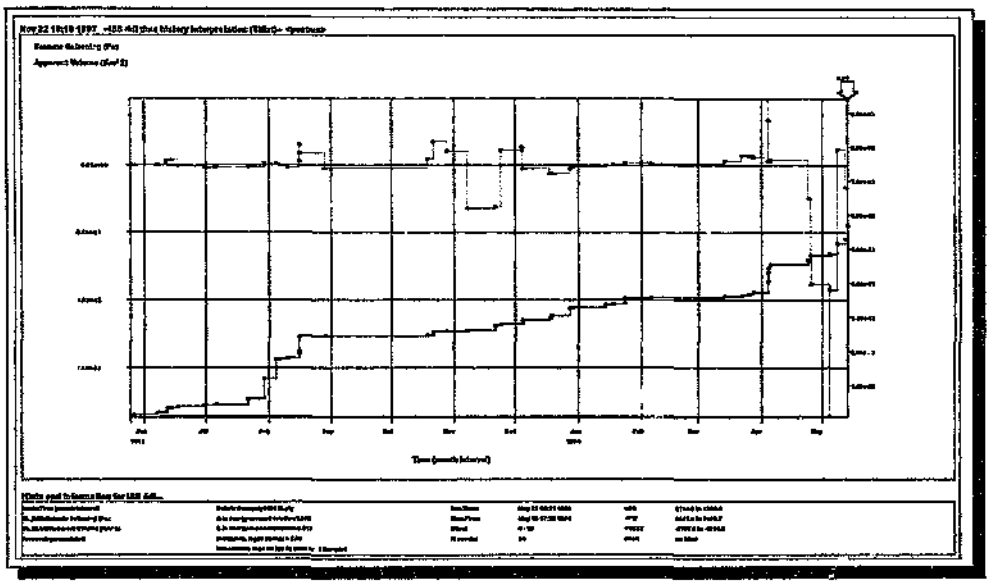

Fig. 4.175: Sensitivity of median seismic softening to a moving window of 5 days and/or 3 samples of data.

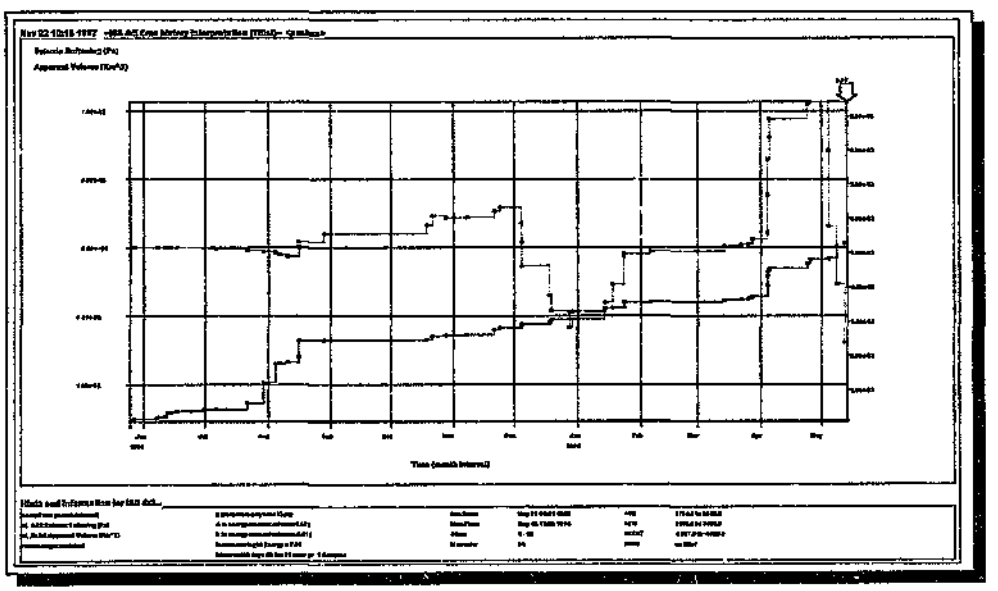

Fig. 4.176: Same as above, but with a moving window of 5 days and/or 7 samples of data.

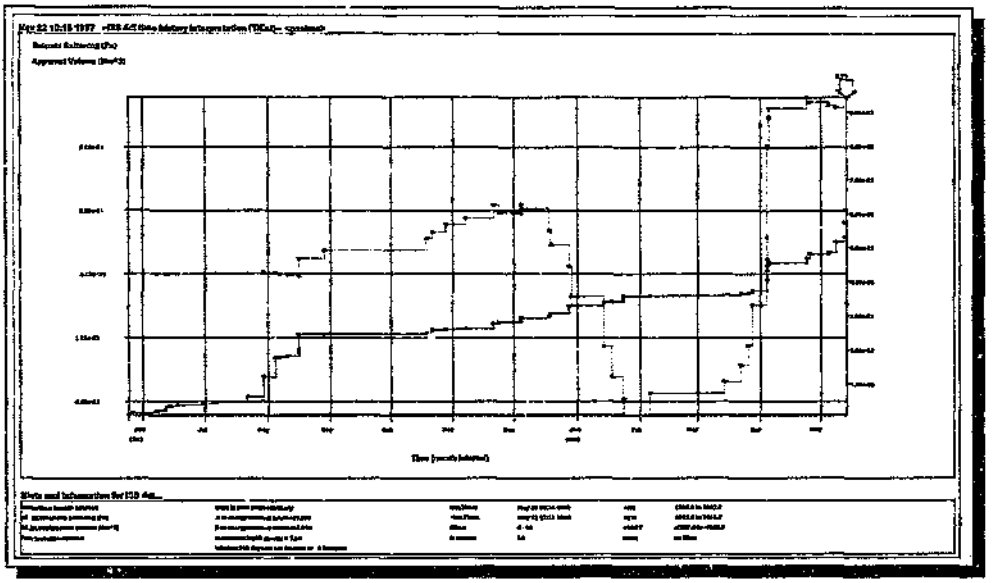

Fig. 4.177: Same as fig. 4.175, but with a moving window of 5 days and/or 9 samples of data.

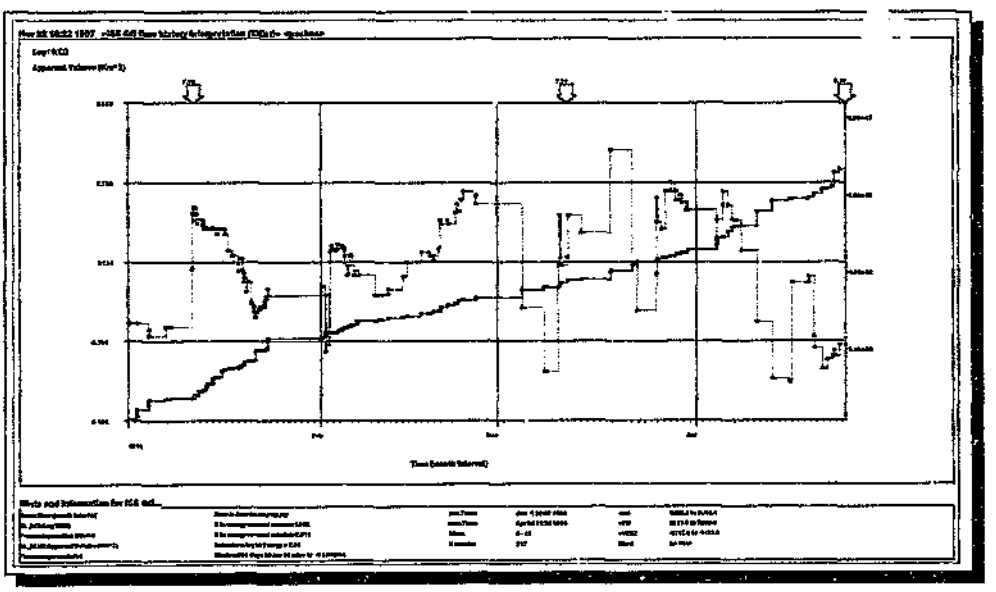

Fig. 4.178: Sensitivity of median log(EI) to a moving window of 5 days and/or 4 samples of data; the time-history of cumulative apparent volume is used as a reference in each subsequent case (figs. 4.179 to 4.198; the time period of seismicity is held constant from 1/1/94 to 24/4/94). The last arrow refers to event 940424.

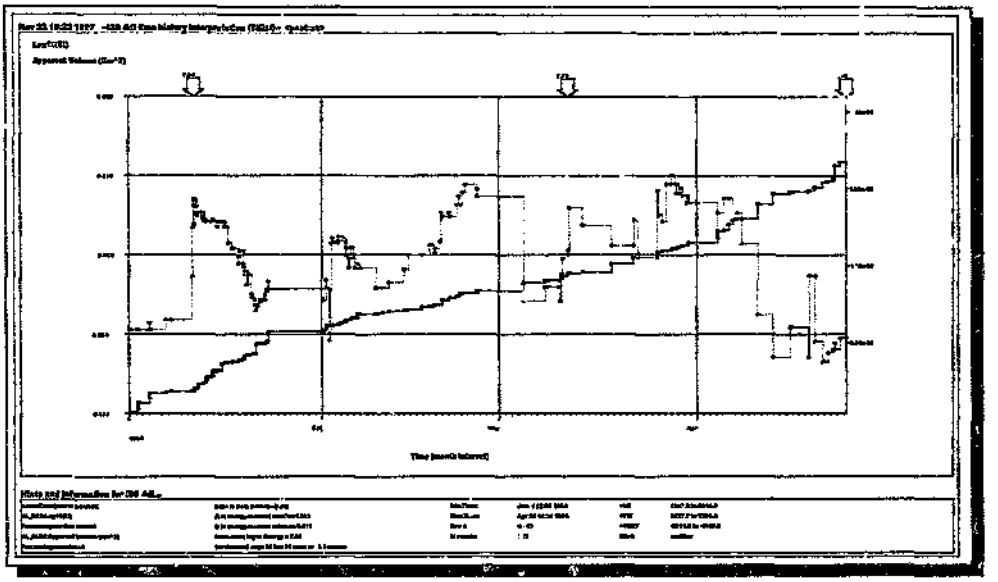

Fig. 4.179: Same as fig. 4.178, but using a moving window of 5 days and/or 6 samples of data.

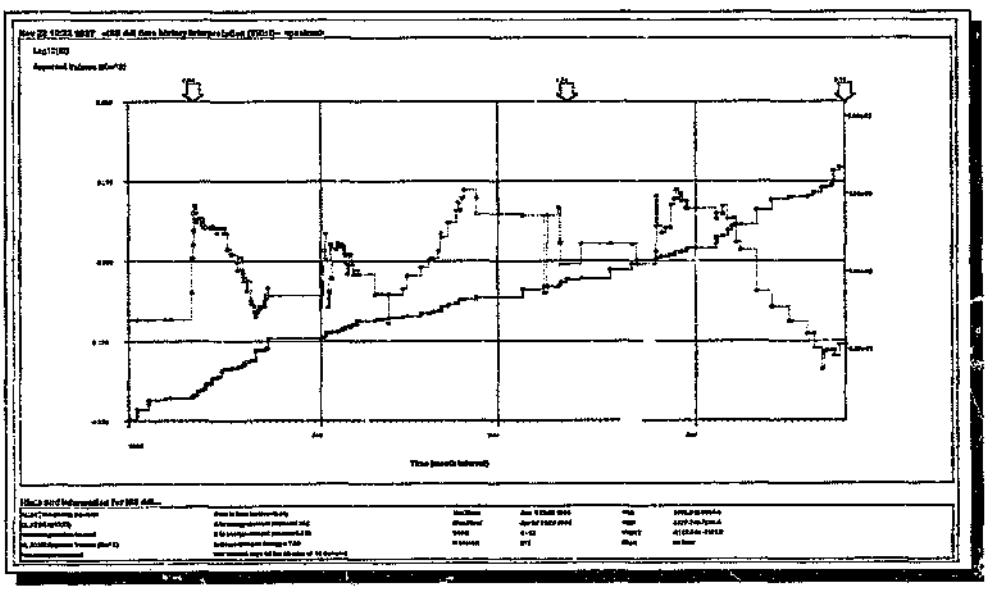

Fig. 4.180: Same as fig. 4.178, but using a moving window of 5 days and/or 10 samples of data.

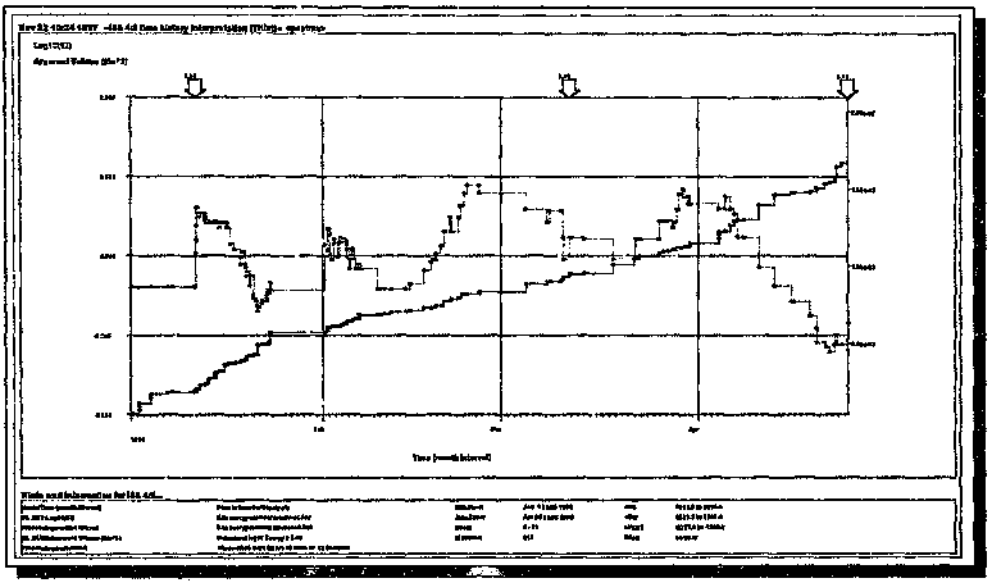

Fig. 4.181: Same as fig. 4.178, but using a moving window of 5 days and/or 12 samples of data.

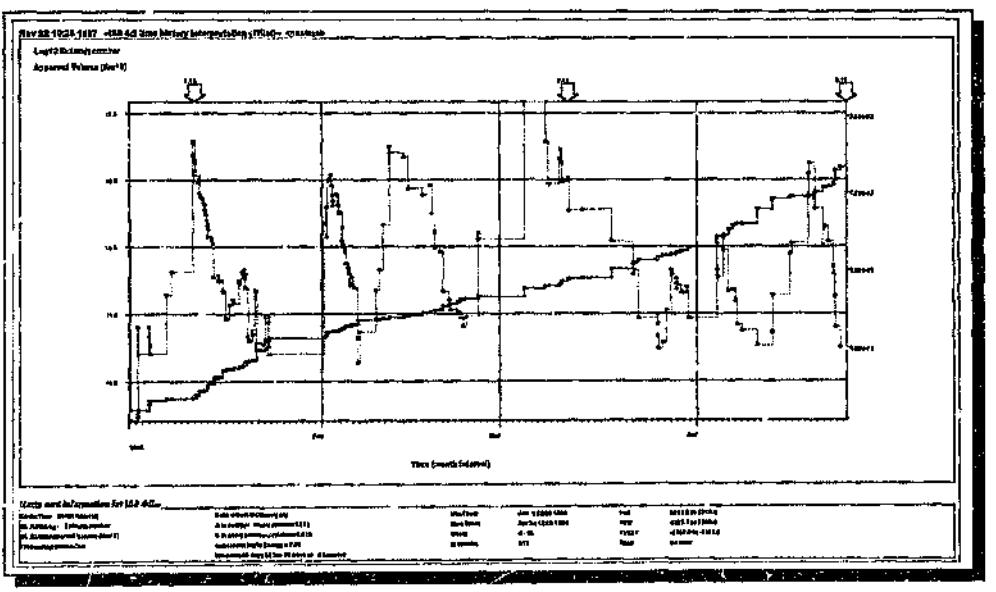

Fig. 4.182: Sensitivity of median log(seismic Schmidt no.) to a moving window of 5 days and/or 4 samples of data.

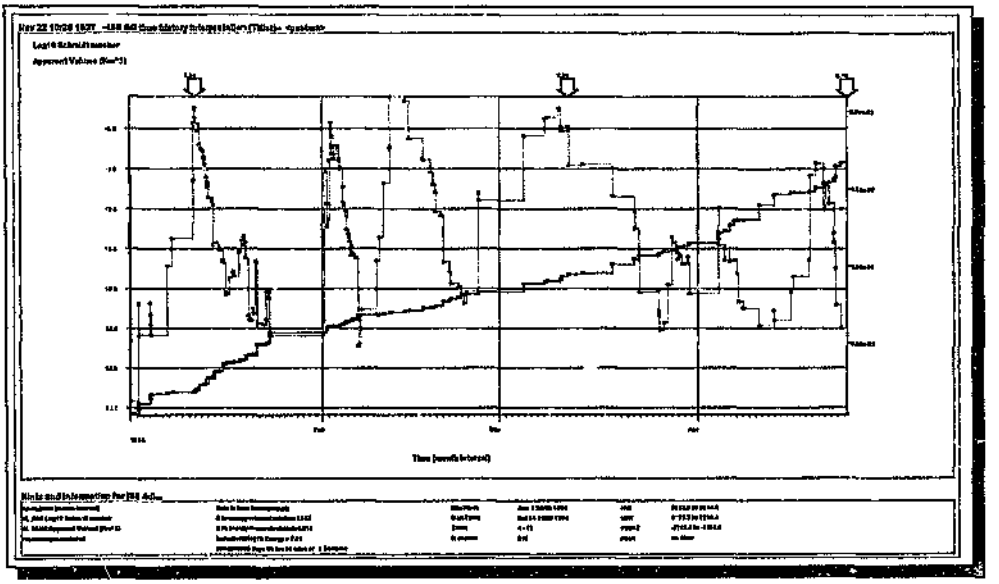

Fig. 4.183: Same as fig. 4.182, but using a moving window of 5 days and/or 6 samples of data.

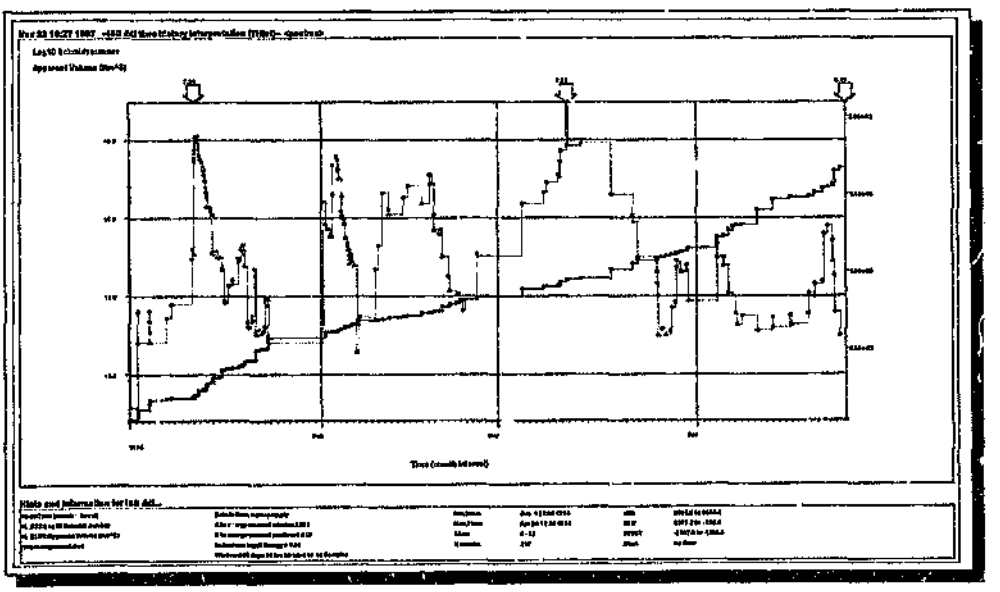

Fig. 4.184: Same as fig. 4.182, but using a moving window of 5 days and/or 10 samples of data.

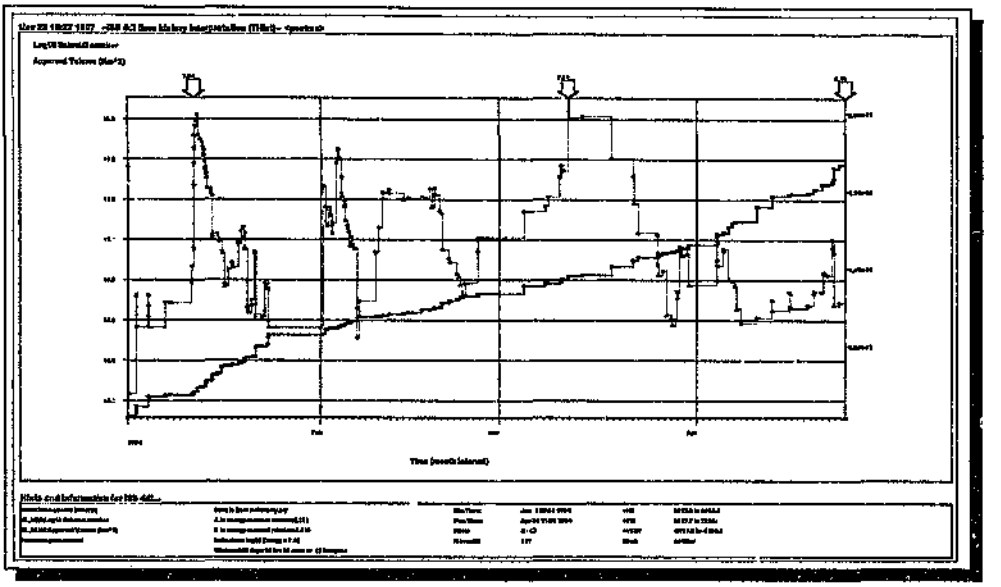

Fig. 4.185: Same as fig. 4.182, but using a moving window of 5 days and/or 12 samples of data.

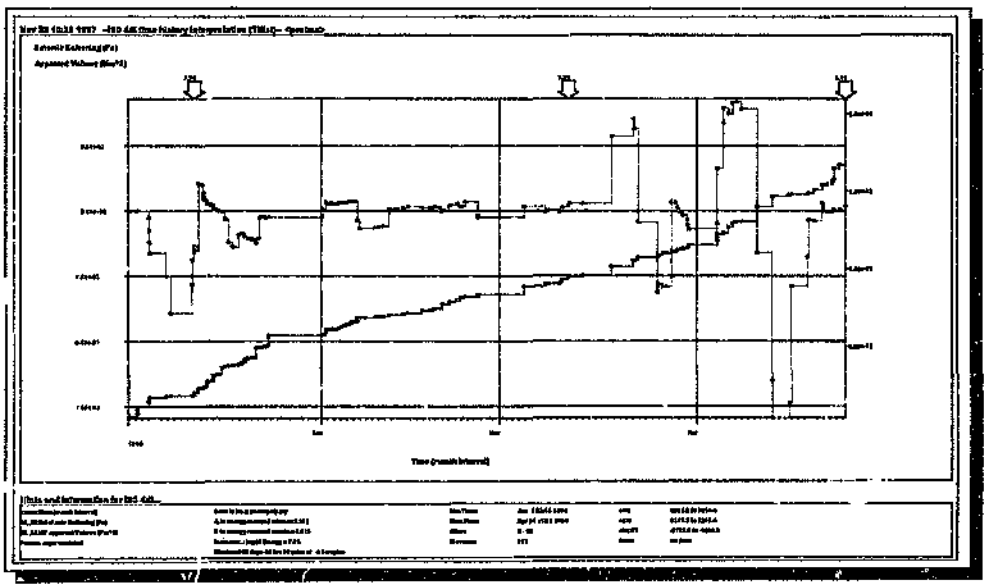

Fig. 4.186: Sensitivity of median seismic softening to a moving window of 5 days and/or 4 samples of data.

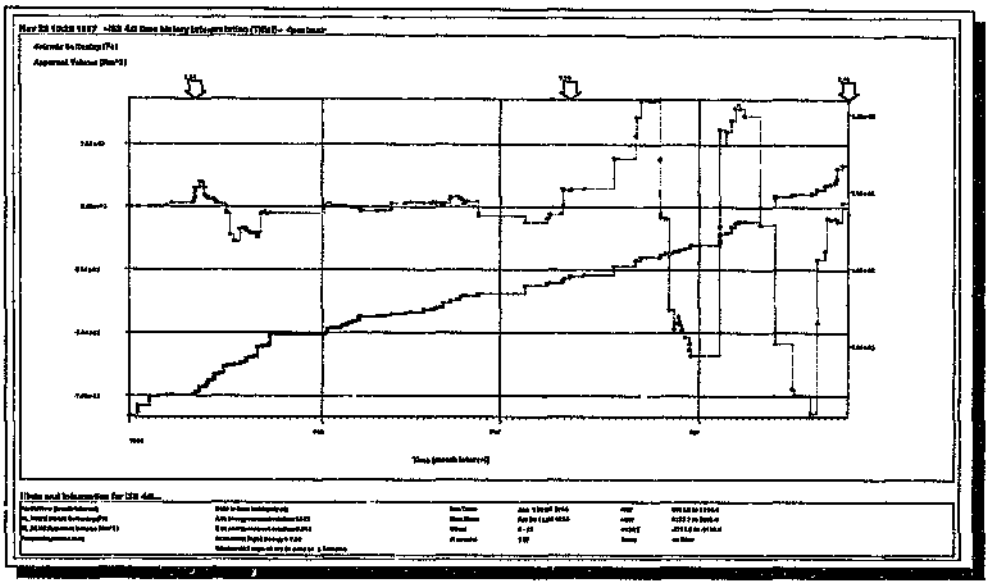

Fig. 4.187: Same as fig. 4.186, but using a moving window of 5 days and/or 6 samples of data.

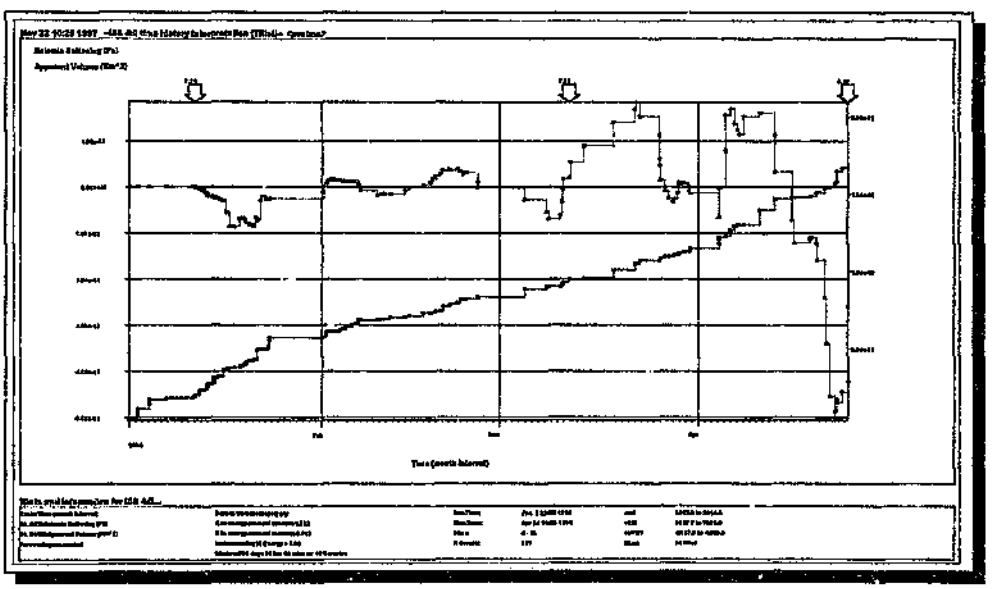

Fig. 4.188: Same as fig. 4.186, but using a moving window of 5 days and/or 10 samples of data.

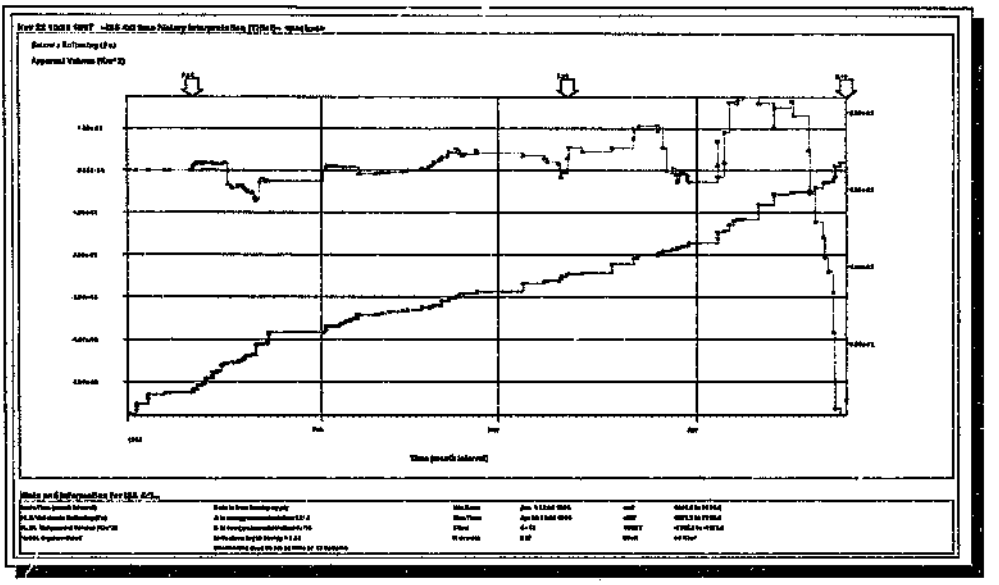

Fig. 4.189: Same as fig. 4.186, but using a moving window of 5 days and/or 12 samples of data.

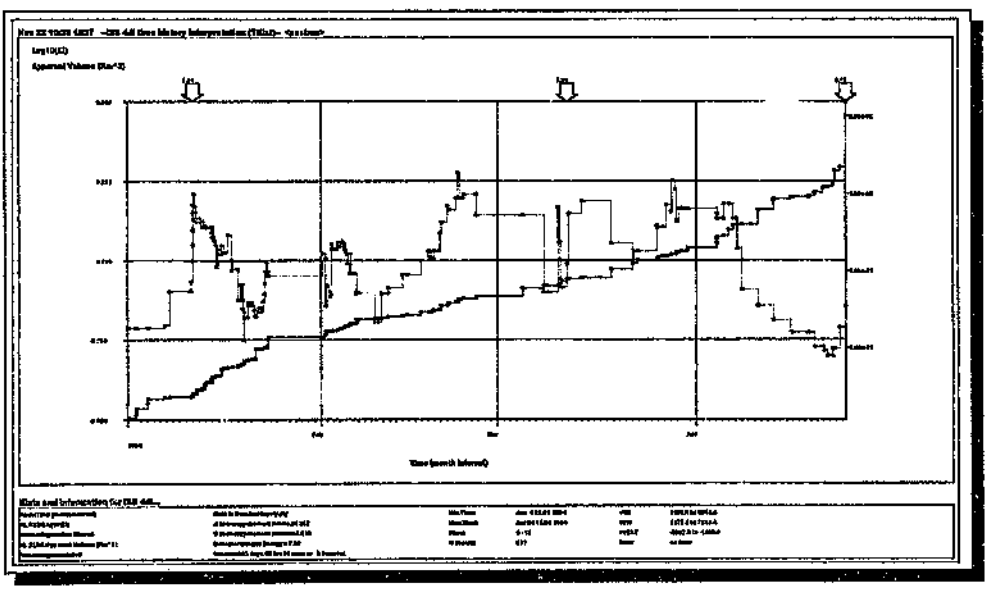

Fig. 4.190: Se itivity of median log(EI) to a moving window of 3 days and/or 8 samples of data.

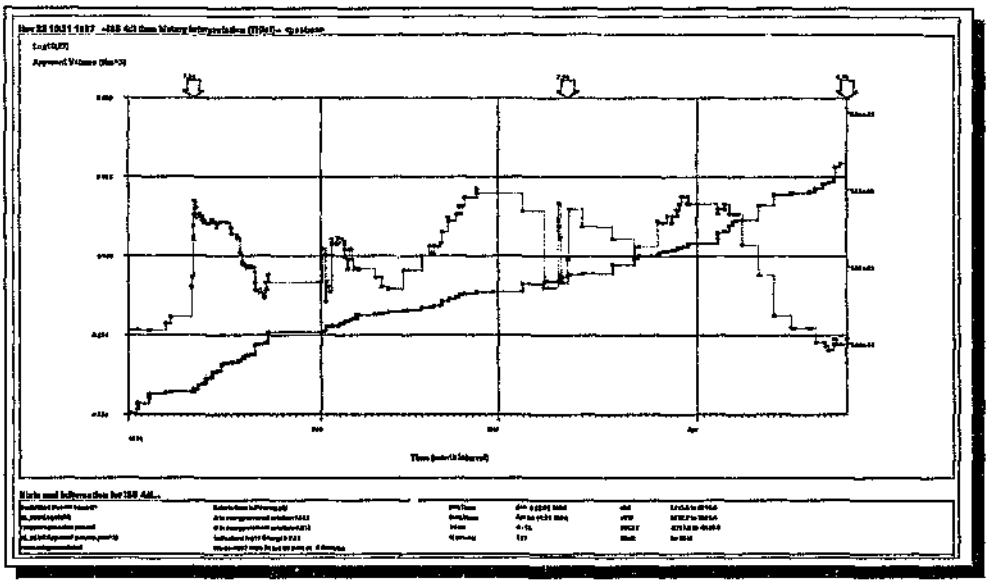

Fig. 4.191: Same as fig. 4.190, but using a moving window of 7 days and/or 8 samples of data.

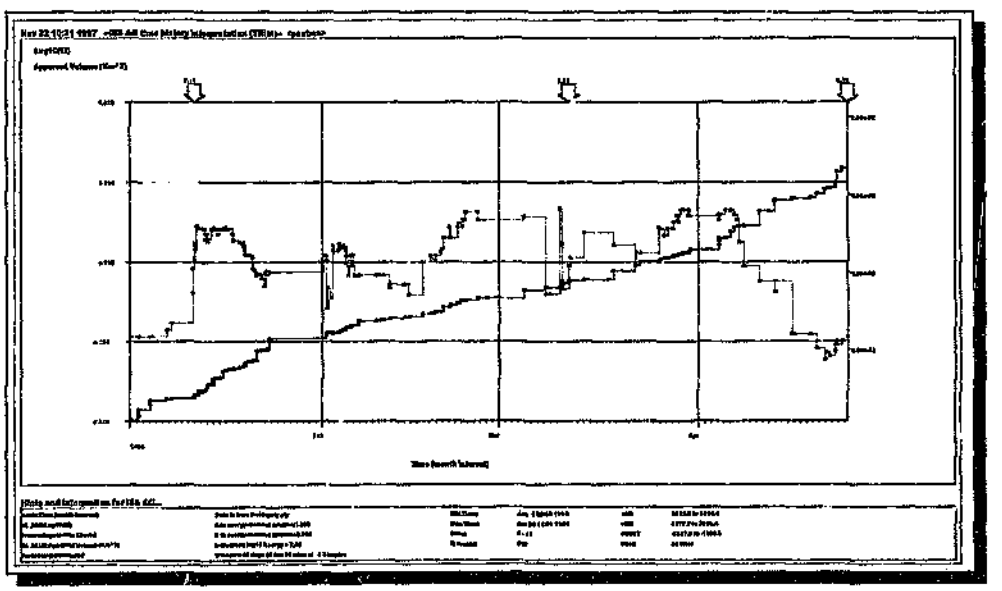

Fig. 4.192: Same as fig. 4.190, but using a moving window of 9 days and/or 8 samples of data.

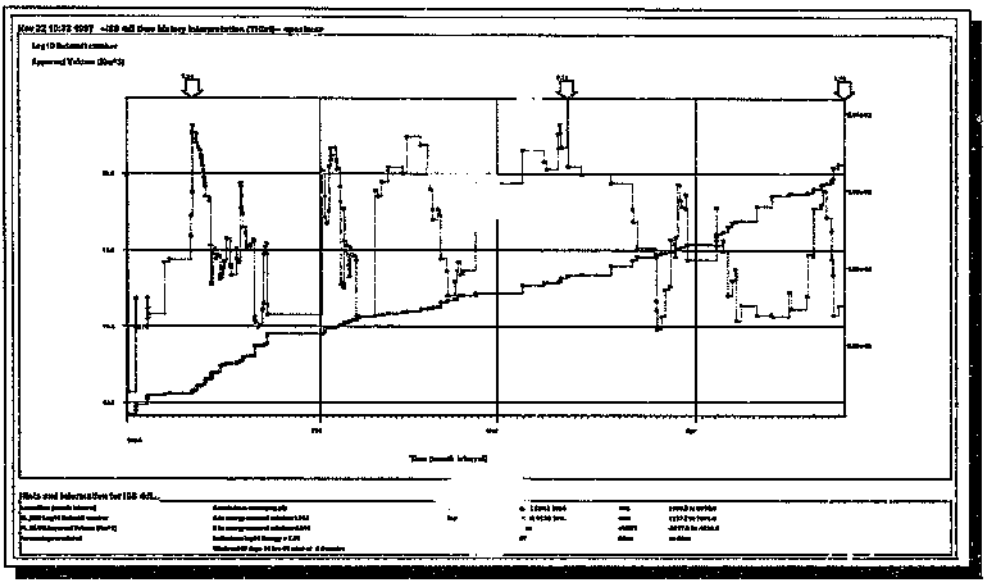

Fig. 4.193: Sensitivity of median log(seismic Schmidt no.) to a moving window of 3 days and/or 8 samples of data.

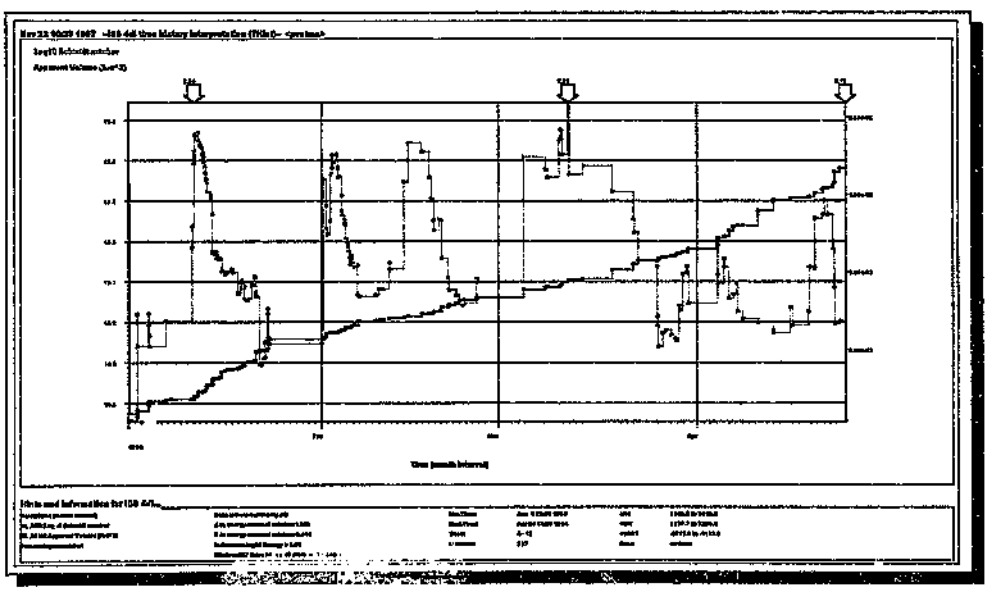

Fig. 4.194: Same as fig. 4.193, but using a moving window of 7 days and/or 8 samples of data.

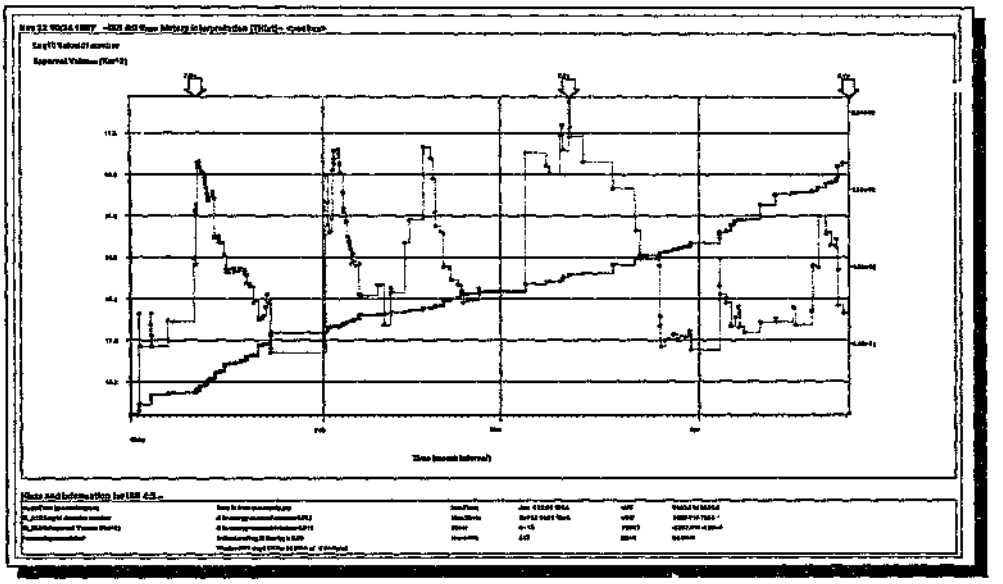

Fig. 4.195: Same as fig. 4.193, but using a moving window of 9 days and/or 8 samples of data.

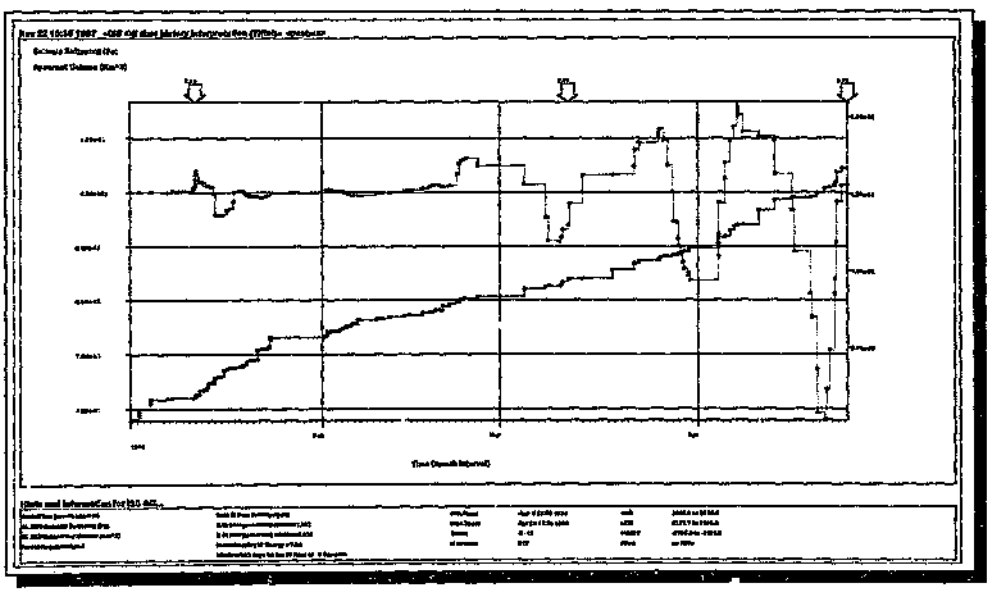

Fig. 4.196: Sensitivity of median seismic softening to a moving window of 3 days and/or 8 samples of data.

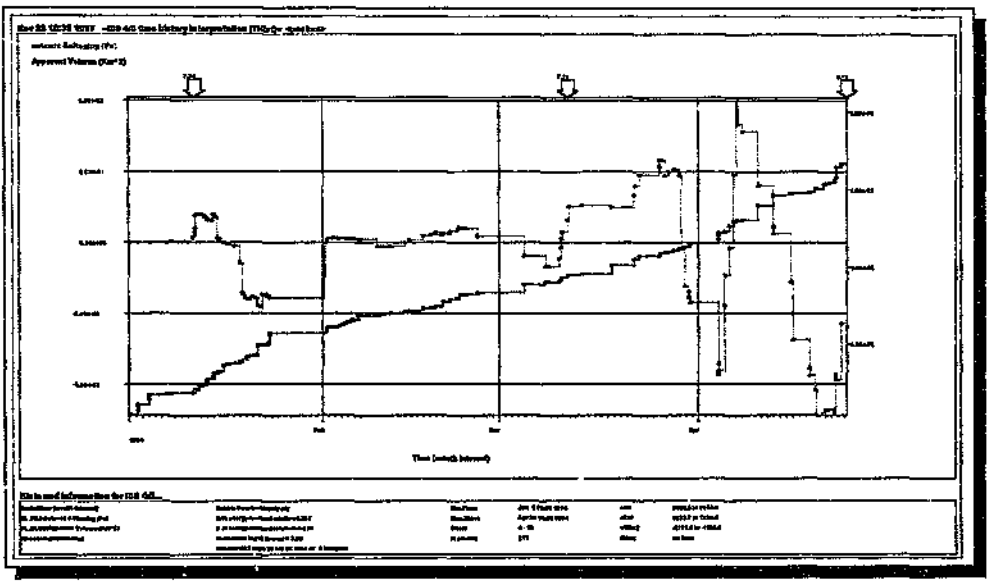

Fig. 4.197: Same as fig. 4.196, but using a moving window of 7 days and/or 8 samples of data.

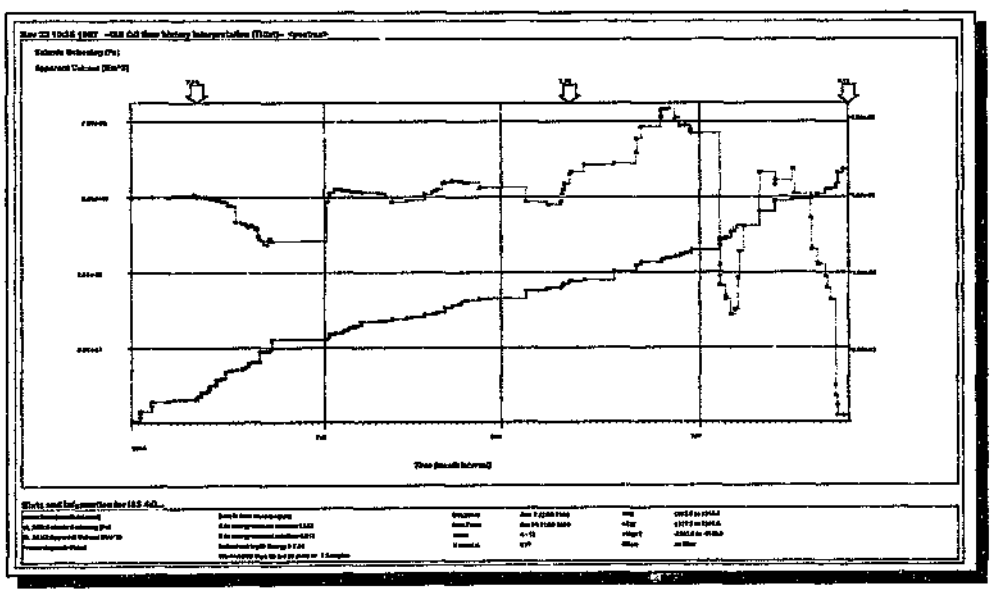

Fig. 4.198: Same as fig. 4.196, but using a moving window of 9 days and/or 8 samples of data.

APPENDIX H

Clustering of seismicity immediately before the occurrence of a large event (figs. 4.199 - 4.205); Section 4.3, Chapter 4.

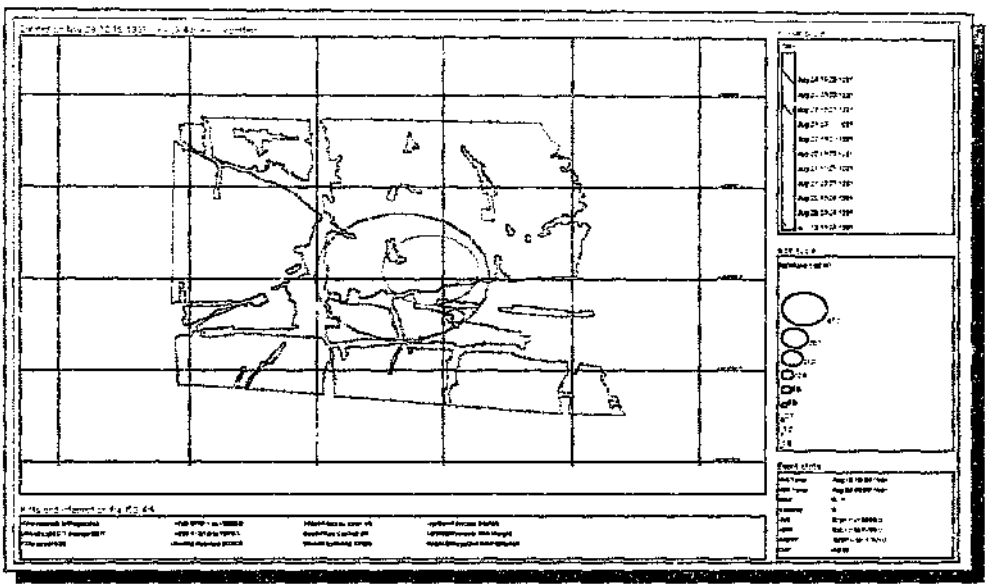

Fig. 4.199: Distribution of recorded seismicity 6 days before (and including) event 910825, which is denoted by the largest symbol. The location of event 910825 lies close to where the other events occurred on plan.

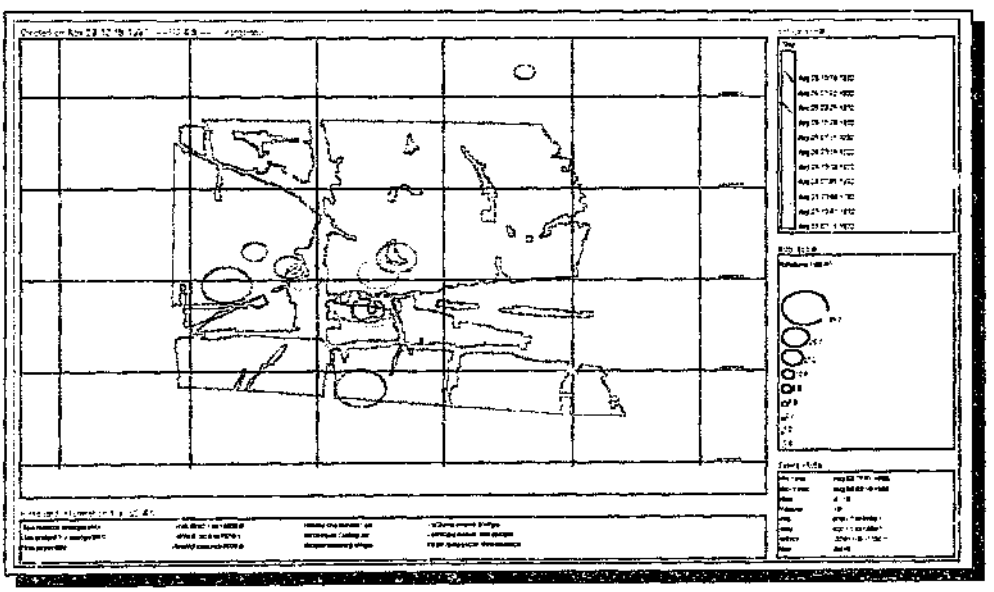

Fig. 4.200: Distribution of recorded seismicity 3 days before (and including) events 920826a and 920826b. Event 920826b (largest symbol), in particular, is preceded by a number of smaller events close to its locality.

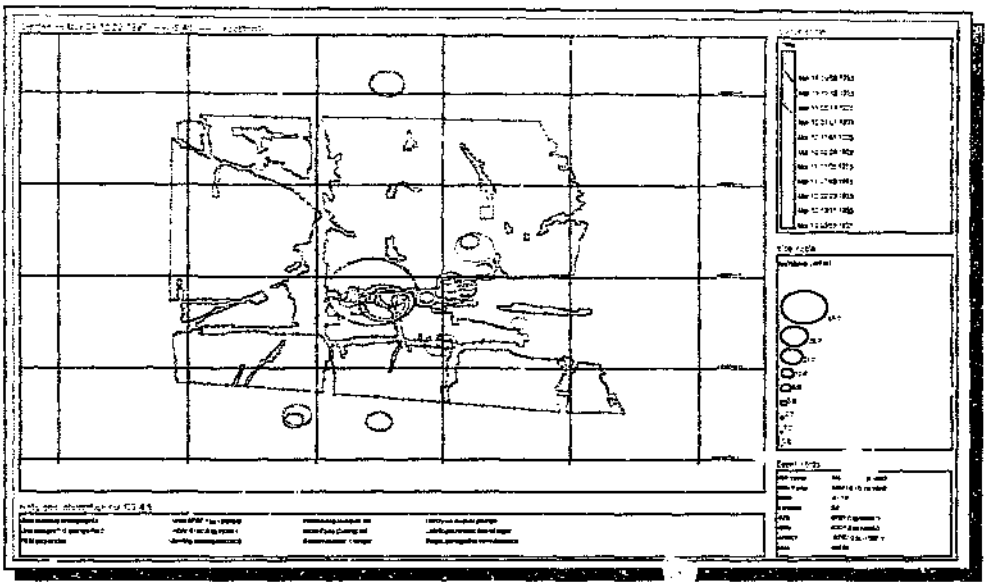

Fig. 4.201: Distribution of recorded seismicity 4 days before (and including) event 930314 (which is denoted by the largest symbol). Note the clustering of preceding, smaller events close to its locality.

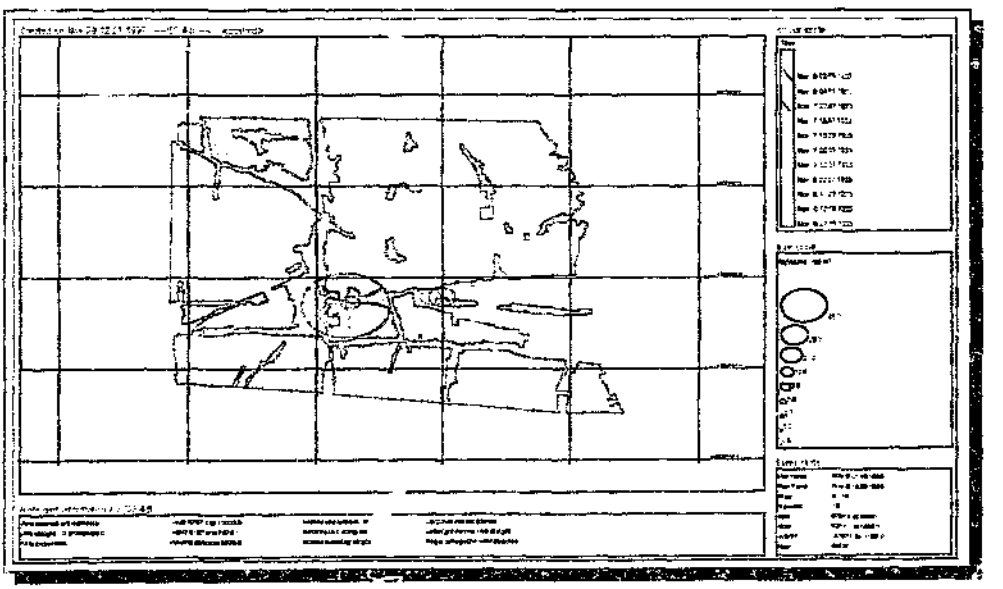

Fig. 4.202: Distribution of recorded seismicity 2 days before (and including) event 931108 (which is denoted by the largest symbol). Again, note the number of smaller, preceding events close to the focus of event 931108.

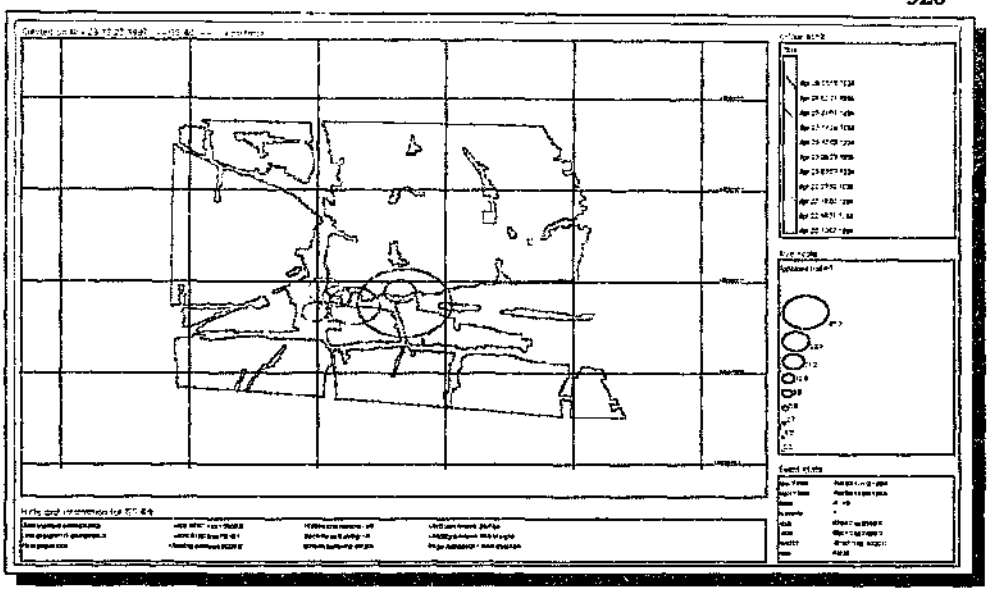

Fig. 4.203: Distribution of recorded seismicity 2 days before (and including) event 940424 (which is denoted by the largest symbol). The latter lies near the edge of the preceding cluster of seismicity.

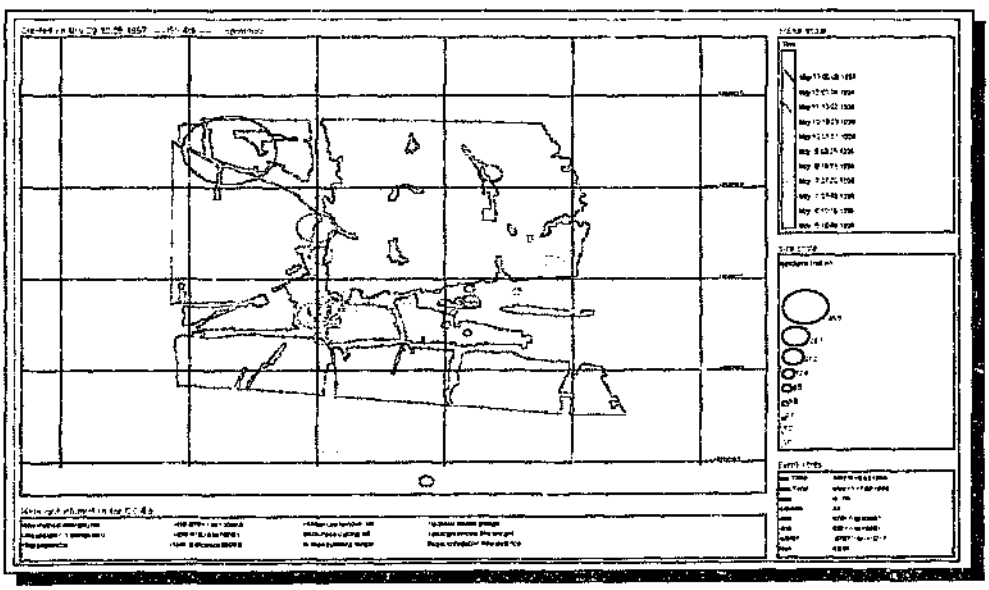

Fig. 4.204: Distribution of recorded seismicity 9 days before (and including) event 940513 (denoted by the largest symbol). In this case, event 940513 is spatially removed from other events; no preceding seismicity was recorded in its immediate environs.

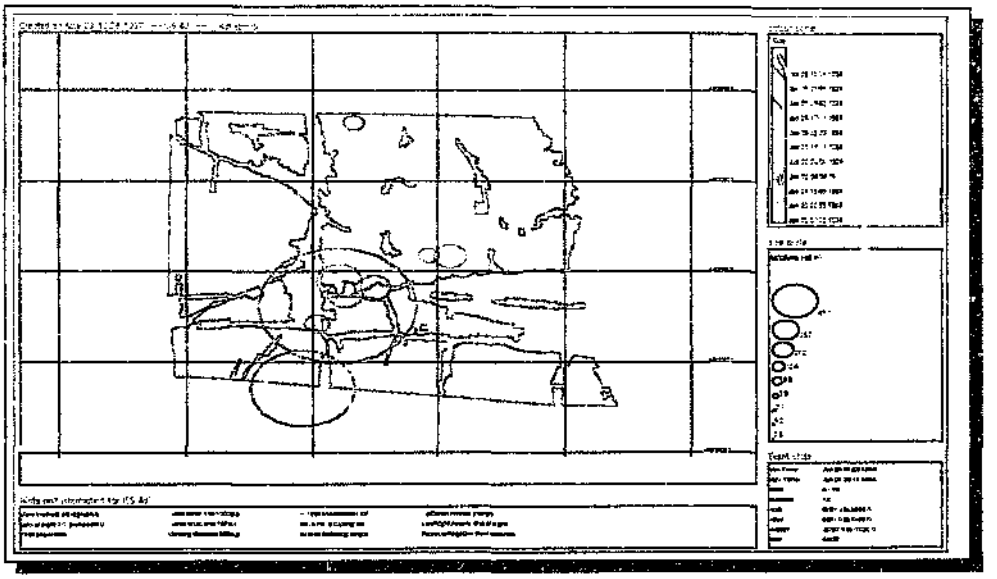

Fig. 4.205: Distribution of recorded seismicity 7 days before (and including) events 940627a (largest symbol) and 940627b (second-largest sysmbol). Event 940627a, close to the fault-dyke intersection, is preceded by a number of smaller events at that locality.

APPENDIX F

Energy indicators used as 'likelihood indicators' of imminent instability (figs. 4.206 - 4.211).

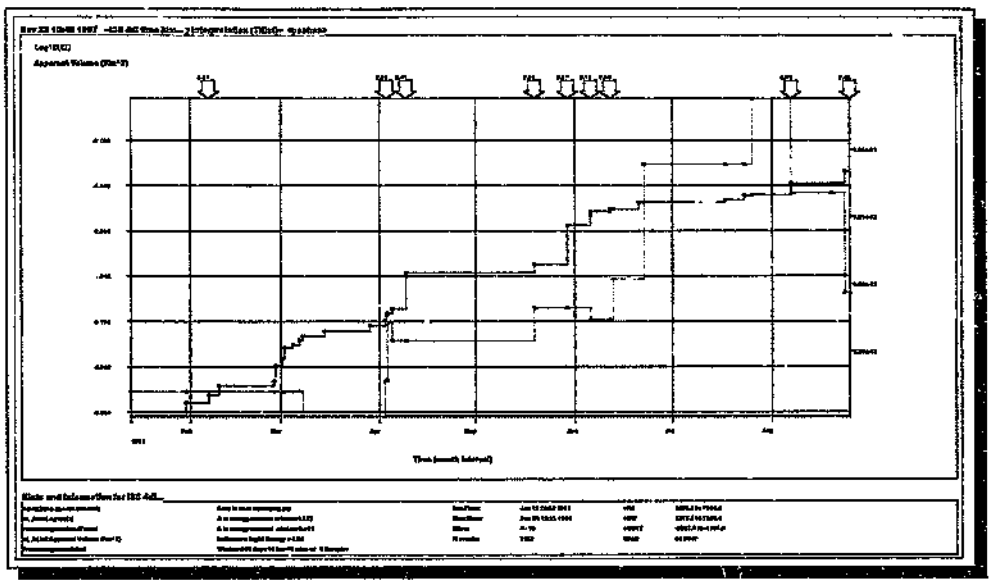

Fig. 4.206: Time-history of cumulative apparent volume and moving median log(EI) for the seismicity associated with the Postma area (January to August 1991, up to and including event 910825). The arrows refer to large events (log(E) > 6.0) whose frequency of occurrence is often quite regular; an absense of larger events would be accompanied by 'gaps' between the arrows. Provided mining continues, the time length of these gaps may be linked to an increasing likelihood of instability.

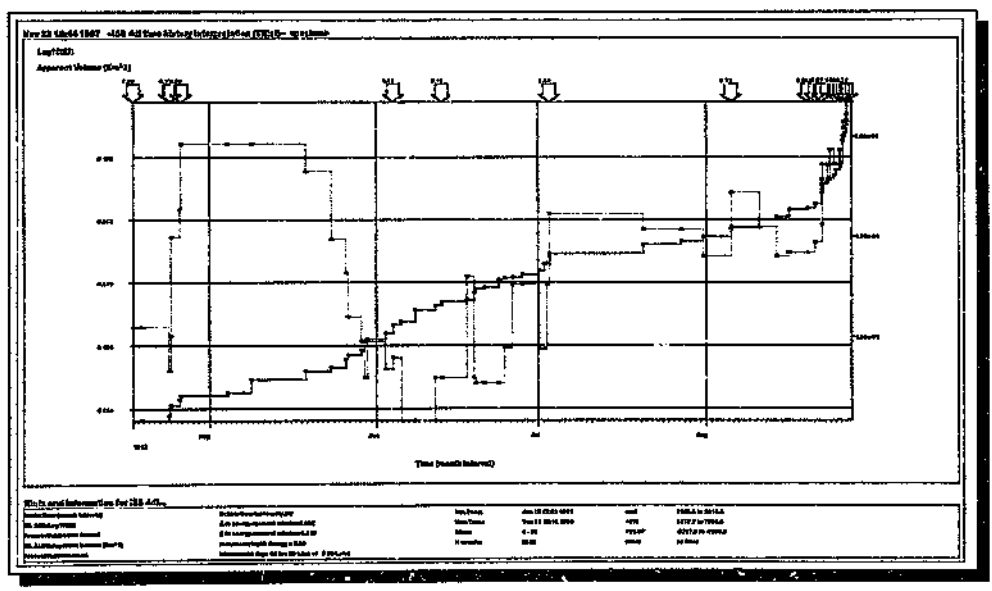

Fig. 4.207: Similar to fig. 4.206; the time period of recorded seismicity is from April to August 1992 (up to and including events 920826a and 920826b).

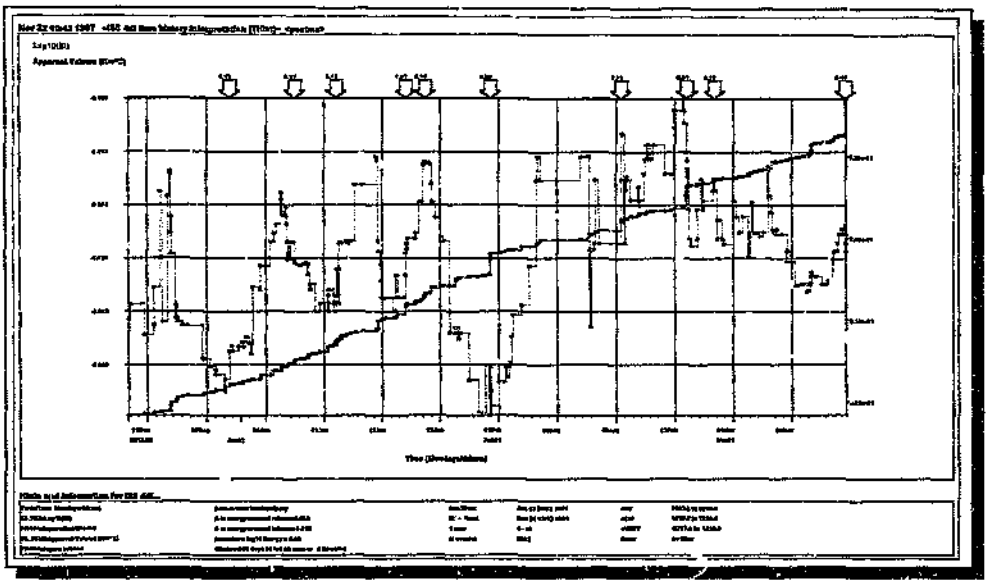

Fig. 4.208: Similar to fig. 4.206; time period of recorded seismicity is from December 1992 to March 1993 (up to and including event 930314).

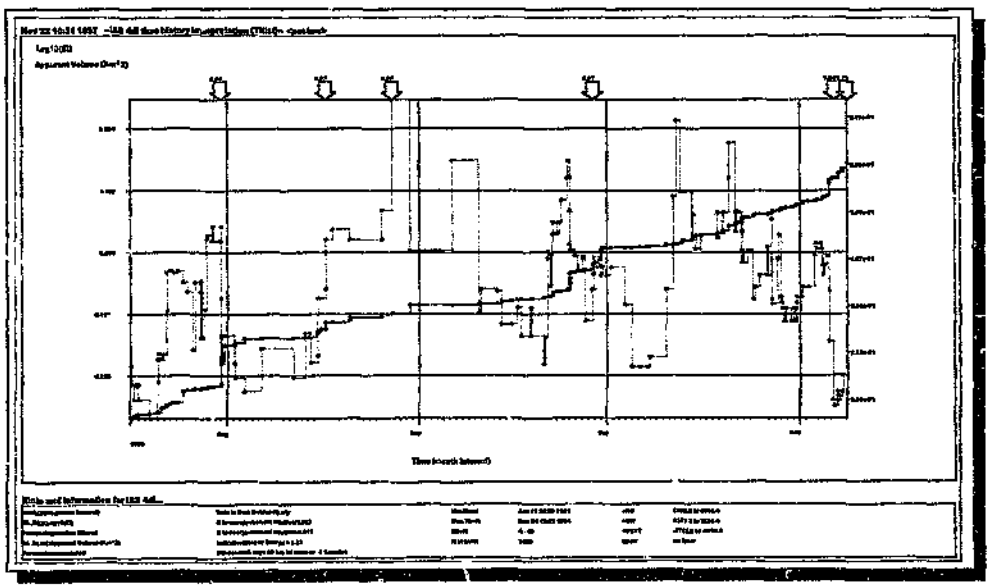

Fig. 4.209: Similar to fig. 4 206; time period of recorded seismicity is from July to November 1993 (up to and including event 931108).

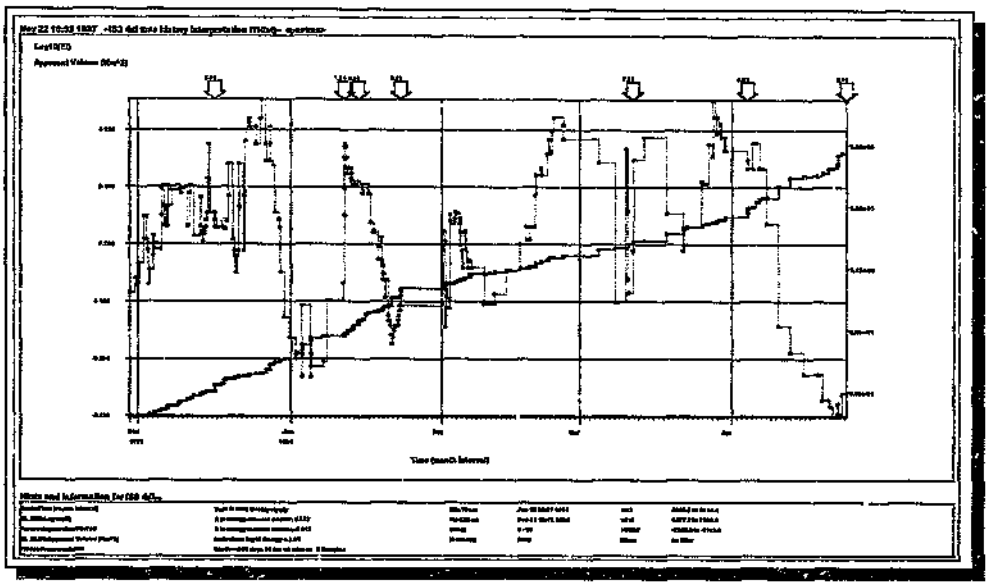

Fig. 4.210: Similar to fig. 4.206; the time period of recorded seismicity is from December 1993 to April 1994 (up to and including event 940424).

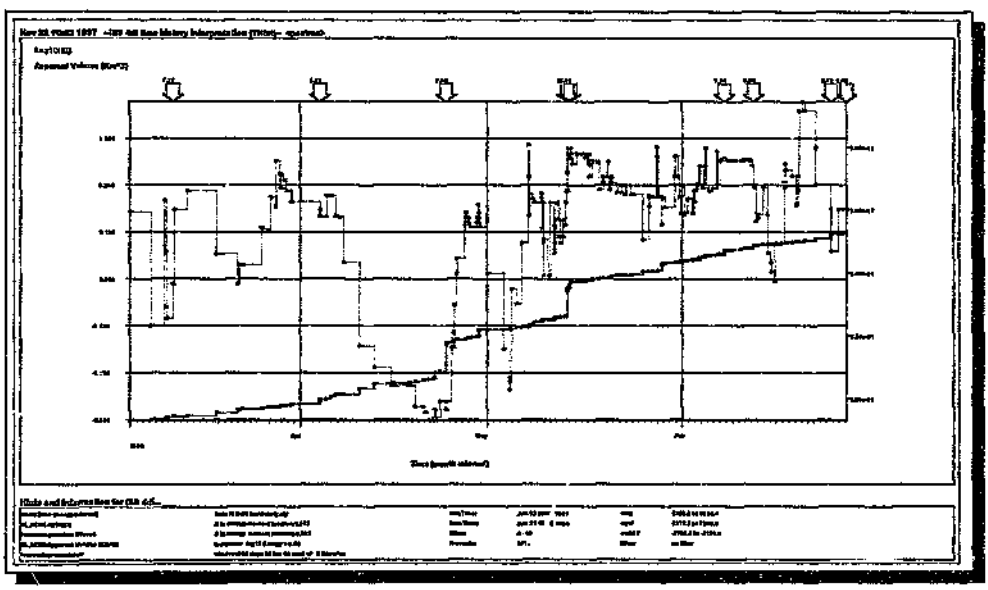

Fig. 4.211: Similar to fig. 4.206; the time period of recorded seismicity is from March to June 1994 (up to and including event 940627a). Note the almost regular occurrence of the larger events, as indicated by the arrows, in this time period.